

DESY SR-74/10
June 1974

DESY-Bibliothek
16. JULI 1974

Vacuum Ultraviolet and Electron Energy Loss Spectroscopy
of Gaseous and Solid Organic Compounds

by

E. E. Koch and A. Otto

Sektion Physik der Universität München, München

To be sure that your preprints are promptly included in the
HIGH ENERGY PHYSICS INDEX ,
send them to the following address (if possible by air mail) :

DESY
Bibliothek
2 Hamburg 52
Notkestieg 1
Germany

VACUUM ULTRAVIOLET AND ELECTRON ENERGY LOSS SPECTROSCOPY
OF GASEOUS AND SOLID ORGANIC COMPOUNDS[†]

E.E. Koch and A. Otto

Sektion Physik der Universität München, München

The experimental arrangements used by the authors for the study of optical vacuum ultraviolet and electron energy loss spectra of organic compounds are described and some theoretical aspects of studies of higher excited states are considered. Results for alkanes, benzene, naphthalene, anthracene and some more complex hydrocarbons are reviewed. Recent results obtained by reflection- and electron energy loss spectroscopy for single crystals of anthracene are included and their relevance for gas phase work as well as for the understanding of exciton effects in organic solids is described.

[†] Dedicated to Prof. Dr. W. Rollwagen on the occasion of his 65th birthday

The authors' research reviewed here was supported, in part, by Deutsche Forschungsgemeinschaft DFG and, in part, by Deutsches Elektronen-Synchrotron DESY

to be published in:

International Journal of Radiation Physics and Chemistry

1. Introduction

Reliable information about vibrational states and the lower energy electronic excitations of organic compounds has been obtained from detailed spectroscopic studies in the infrared and visible range of the spectrum (e.g. Ref. 1,2,3). Comparatively little is known about the higher excited states of such molecules. Although the importance of these states was discussed quite early⁴, investigations for the spectral range 10 eV to 40 eV, where the absorption process has its maximum cross section for a large number of organic compounds, are scarce. This is partly due to the inherent experimental difficulties of spectroscopic work in the vacuum ultraviolet (VUV), such as light source and monochromator design problems in optical experiments or the comparatively low resolution in electron loss spectroscopy. Only recently some of the experimental difficulties have been solved for instance by using synchrotron radiation as an intense source of polarized light or by the introduction of electron spectrometers with high performance monochromators and analyzers. It is anticipated that more studies within the near future will use these tools, stimulating the investigation of higher excited states of many organic compounds, and thereby complementing the results obtained by photoelectron spectroscopy (PES)^{5,6}.

This review is limited in scope primarily to those results obtained by the authors during the last few years from optical and electron loss studies of a number of molecules. Where recent, up-to-date reviews or discussions are available we have tried to avoid duplication of arguments and simply have given appropriate references. We have discussed only those problems which seem most interesting to us. Necessarily this is an arbitrary selection, which reflects our personal interests. The reader interested in more exhaustive reviews is referred to the recent books by Robin⁷ and the summary of lectures given in Ref. 8.

Our experimental arrangement is briefly described in Chapter 2. In Chapter 3 we consider various theoretical aspects and give the rationale for our studies. In particular we discuss the relation between optical absorption and electron loss spectroscopy and comment on the existence of collective excitations in large organic molecules. The following chapters are devoted to a presentation of and some comments on the experimental results obtained for alkanes (Chap. 4), benzene (Chap. 5), naphthalene (Chap. 6), anthracene (Chap. 7) and some more complex molecules (Chap. 8).

Some recent experimental results for VUV excitations in organic molecular crystals, studied by reflection and electron loss spectroscopy, have been included. These experiments were undertaken in order to study the influence of the solid environment on the molecular excitations in weakly-bound van der Waals crystals. In particular, anthracene single crystals have been studied extensively both experimentally and theoretically as prototypes for a large group of molecular crystals.

2. Experimental Methods

2.1 Optical Experiments

In all our optical experiments, the results of which will be discussed in the following sections, synchrotron radiation⁹ from the electron accelerator DESY served as intense polarized light. Its spectral distribution is continuous. Since experimental aspects of vacuum ultraviolet spectroscopy in general have been described in text books^{10,11}, and general aspects of practical work with synchrotron radiation have been reviewed previously¹²⁻¹⁶, only a brief description of the apparatus used in our studies is given here.

The continuous spectrum of synchrotron radiation, which is emitted from the electrons within the accelerator, is monochromatized by near normal incidence (visible to 45 eV range) or grazing incidence (25 eV to 500 eV range) monochromators, depending on the spectral range of interest. Valence electron excitations in organic molecules and molecular crystals can be studied conveniently with normal incidence monochromators. An instrument especially suited for work with synchrotron light is sketched in Fig. 1 and Fig. 2¹⁷. It operates without entrance slits in a modified Wadsworth mount¹⁸, taking advantage of a dispersion plane perpendicular to the synchrotron plane. Since the vertical extension of the electron beam in the synchrotron is smaller (≈ 2 mm) than the horizontal extension (≈ 10 mm), the resolution in the vertical Wadsworth mounting is better than that obtained with a horizontal dispersion plane. Furthermore since the planes of incidence of the premirror as well as that of the grating are perpendicular to the synchrotron plane (see Fig. 2), this arrangement yields an even higher degree of polarization. With a 2400 lines/mm grating and 250 μ slit width of the exit slit, a spectral resolution of better than 1 \AA (30 mV at 20 eV) over the whole spectral range from 5 to 45 eV is obtained. Behind the exit slit a photon flux of 3×10^9 photons/ \AA ·sec, as measured by a double ionization chamber¹⁹, is

obtained at 600 Å (≈ 20.66 eV) under typical working conditions of the accelerator (4.5 GeV, 30 mA).

Either a windowless absorption chamber for gas phase work (Fig. 1) or an ultrahigh vacuum chamber for reflection experiments on solid samples (Fig. 2) may be attached at the exit arm of the instrument. Reflection spectroscopy is employed for the study of the optical properties of solid samples in the VUV range, because even with intense light sources and very thin crystals the absorption of almost all substances in this range is too strong. This is not a severe restriction, because one can obtain the same information via Kramers-Kronig analysis of reflectance spectra. It has been shown recently²⁰ that even for anisotropic monoclinic crystals normal incidence reflectance measurements for a small number of particular polarization directions suffice to deduce the full information about the dielectric tensor.

Polycrystalline films, vacuum-deposited on a cooled substrate can be investigated in slightly modified experimental arrangements. In such reflection experiments the optical properties of solid samples of compounds volatile at room temperature (rare gases²¹⁻²³ atmospheric gases^{24,25}, alkanes²⁶) have been studied. The synchrotron "light bulb" is very well suited for all these experiments.²⁷ The high intensity allows for photoelectric recording of absorption spectra; the high degree of polarization makes it an excellent source for measurements on anisotropic single crystals, and the low base pressure within the accelerator minimizes problems of differential pumping in cryoexperiments in order to avoid surface contamination.

In connection with grazing incidence instruments, it is possible to extend the studies to core level excitations. In particular, investigations of the carbon K_{1s} edge (~ 290 eV) of organic compounds seem desirable. However,

except for a pilot experiment on methane²⁸ practically no work has been done so far in this range.

2.2 Electron energy loss experiments

In electron energy loss spectroscopy, electrons rather than photons are used to excite the electronic transitions. Electrons with fixed initial energy, monochromatized by an electron monochromator or with an energy spread characteristic of the thermal emission from the cathode, are scattered inelastically in the target chamber or in the sample foil. The characteristic energy loss of the electron scattered in a particular direction is detected with an electron analyser, the electron energy loss ΔE being equal to an excitation energy of the scatterer. In this type of experiment the direction and magnitude of the wave vector \underline{k} for the excitation may be chosen nearly independently from the excitation energy. This is an advantage over optical experiments where $|\underline{k}| \approx 0$.

The experimental and theoretical aspects of molecular spectroscopy with electrons of moderate kinetic energy (several 100 eV) have been reviewed by Lassette and coworkers^{29,30}. For the investigation of solid films, higher kinetic energies are necessary in order to penetrate the sample. Aspects of this particular kind of electron loss spectroscopy on solids with fast electrons (30 - 60 keV) have been described in several reviews³¹⁻³³.

Again only the apparatus used for studies on organic compounds in our laboratory (Fig. 3) will be described³⁴⁻³⁹. It is adequate for studies of electron loss spectra of fast electrons (30 keV) from both vapor phase and solid samples. A severe limitation is its low energy resolution, because no electron monochromator is employed. The electron beam is focused onto the entrance slit of the analyser. The target holder (OS) for investigations of thin foils can be

cooled to 170 K. Furthermore it is adjustable by displacement in a plane perpendicular to the electron beam and by rotation around axes perpendicular and parallel to the beam. The adjustment of the crystal axes into definite positions with respect to the beam is controlled by the recognition of the known electron diffraction patterns³⁴. The electron loss spectra from this target or from vapours enclosed in the bakeable collision chamber (OV) are observed in transmission with a Möllenstedt analyser. The energy resolution is about 0.7 eV, the angular resolution $\Delta\theta = \pm 1.5 \cdot 10^{-4}$ rad. For spectroscopy on single crystals, spectra were measured for different scattering angles θ using the calibrated angular deflection system (ESA). Electron detection is either accomplished by a fluorescence screen with photomultiplier and DC-recording or by a Si-surface barrier detector and registration with a multichannel analyser³⁹.

3. Theoretical aspects

3.1 Cross section in optical absorption and electron energy loss experiments

Within the first Born approximation the cross section $\sigma(\omega, \underline{k})$ for inelastic electron scattering with energy loss $\hbar\omega$ and momentum transfer $\hbar\underline{k} = \hbar\underline{k}_f - \hbar\underline{k}_i$, where $\hbar\underline{k}_i$ and $\hbar\underline{k}_f$ denote the momentum of the incoming and scattered electron respectively, is given by equation (1), when exchange effects are neglected.^{40,41}

$$\sigma(\omega, \underline{k}) = \frac{2me^4}{\hbar^3\omega} \frac{|\underline{k}_f|}{|\underline{k}_i|} \frac{1}{k^2} f(\omega, \underline{k}) \quad (1)$$

Here $f(\omega, \underline{k})$ is the generalized oscillator strength⁴².

The optical absorption coefficient μ due to dipole excitations is given by (Ref. 42):

$$\mu(\omega) = \frac{2\pi^2 e^2}{mc} \cdot N \cdot f(\omega, 0) \quad (2)$$

where N is the density of the absorbing molecules. Some comments are in order on the dependence of the oscillator strength on the relative orientation of the molecules with respect to the electric vector of the incident radiation \underline{E} and to the direction of \underline{k} in electron energy loss. For experiments on solids these directions are of importance, since the highly anisotropic molecules are fixed in the crystalline array. In a zero order approximation such a crystal may be considered as an oriented gas⁴³.

For optical absorption $f(\omega, 0)$ is given by (Ref. 42):

$$f(\omega, 0) = \frac{2m\omega}{\hbar} |\langle \psi(\omega) | \sum (\underline{r}_i \cdot \hat{\underline{E}}) | \psi(0) \rangle|^2 \quad (3)$$

where $\hat{\underline{E}} = \frac{\underline{E}}{|\underline{E}|}$ is the direction of the electric field vector and $|\psi(0)\rangle$ and $|\psi(\omega)\rangle$ are the ground and excited state of the molecule respectively. The orientation of the molecule is contained in $|\psi(0)\rangle$ and $|\psi(\omega)\rangle$.

For inelastic electron scattering the cross section $f(\omega, \underline{k})$ is given by (Ref. 41):

$$f(\omega, \underline{k}) = \frac{2m\omega}{\hbar} |\langle \psi(\omega) | \sum e^{i\underline{k}r_i} | \psi(0) \rangle|^2 \quad (4)$$

For $\underline{k} \rightarrow 0$ this yields

$$f(\omega, 0) = \frac{2m\omega}{\hbar} |\langle \psi(\omega) | \sum (\underline{r}_i \cdot \hat{\underline{k}}) | \psi(0) \rangle|^2 \quad (5)$$

From equation (3) and (5) it follows that the direction $\hat{\underline{E}}$ of the electric field in optical absorption corresponds to the direction of momentum transfer $\hat{\underline{k}} = \frac{\underline{k}}{|\underline{k}|}$ in inelastic electron scattering. For forward scattering of the electrons, \underline{k} is very small ($\underline{k} = \frac{\omega}{v^2} \underline{v}$, where \underline{v} is the velocity of the scattered electron). In this case the cross section eq. (1) contains the same $f(\omega, 0)$ - spectrum as the optical absorption spectrum (eq. 2). This is the so-called "optical approximation" in inelastic electron scattering.

For a comparison of the forward scattering spectra $\sigma_f(\omega)$ with optical absorption spectra $\mu(\omega)$, we proceeded in the following way:

The spectrum $\sigma_f(\omega)$ has to be corrected by the frequency dependent factor

$$F(\omega) = \left(\ln \left(1 + \frac{4E^2 \Delta\Theta^2}{(\hbar\omega)^2} \right) \right)^{-1} \quad (6)$$

where $\Delta\Theta$ is the halfwidth of the experimental angular spread of the electron beam and E is the kinetic energy of the incident electrons. Spectra corrected in this way should be proportional to $\mu(\omega)$ spectra.

As an example, the optical absorption cross section and the corrected inelastic electron scattering cross section $\sigma_f(\omega)$ for benzene are compared in Fig. 4. A prescription for obtaining the generalized oscillator strength from energy loss spectra has been given by Lassette^{29,30}.

3.2 Collective effects

Some authors have argued that inelastic electron scattering would be the appropriate method to probe for collective effects in molecules⁴⁴. The argument is essentially the following. Plasmons in metals are detected as maxima in inelastic electron scattering spectra, whereas they do not couple to normal incidence radiation. In analogy one should probe for collective effects in molecules by inelastic electron scattering.

However, this analogy to solids does not exist. According to the previous section, the absorption and inelastic forward scattering spectra for gaseous samples are equivalent. Therefore one cannot assign collective excitations in molecules by looking for structures in inelastic energy loss spectra, which one expects to be missing in optical absorption.

The reason for the different behaviour of molecules and solids in this regard is the following. In solids, the long range collective effects are due to long range interactions. On a small molecule there are, because of the small extension, a priori no long range interactions. Only for molecules, which are kept in crystalline order, do long range intermolecular interactions occur, and subsequently, electron loss spectra with small k and optical absorption spectra, both measured for the crystal, become different, as discussed in the next section.

There is, on the other hand, a gradual transition between collective excitations and single particle excitations for solids. For aluminum plasmon like resonances may be monitored up to $k = 2 \text{ \AA}^{-1}$ ⁴⁵, which corresponds to $\lambda = \frac{2\pi}{k} = 3.14 \text{ \AA}$. This resonance is very highly damped. From both facts one may conclude that only a few neighbouring electrons are involved in this type of collective excitation. The λ value as well as the small number of electrons are within the dimensions of a larger organic molecule.

Therefore we conjecture that collective excitations should show up as resonances in the generalized oscillator strength at large \underline{k} . Experimentally, this will be difficult to observe, since $\sigma(\omega, \underline{k})$ decreases quadratically with \underline{k} (equation (1)). No experimental results relevant to this problem are known to the authors.

Theoretical work on collective effects in atoms and molecules has to consider electron correlation effects. Whereas a large number of studies has been devoted to electron correlation effects in atoms⁴⁶⁻⁴⁸, less work has been done for the same effects in molecules.

Herzenberg et al.⁴⁹ considered the influence of dipole-dipole interactions on the excitation spectrum of ethylene. According to their calculations the $\pi-\pi^*$ singlet and triplet states are shifted in energy and an isolated collective singlet state is predicted at 50 eV. However, spectra obtained by Lee et al.⁵⁰ for this energy range provide no evidence for this state.

In contrast to the conclusions in Ref. 49 Gutfreund and Little⁴⁴ predicted that the highest excitation due to the π -electrons in hexabenzocoronene is only ~ 0.5 eV above the highest Hückel excitation energy. Rather than giving rise to an isolated collective excitation, the electron electron interaction strongly enhances the oscillator strength at the upper edge of the band of single particle excitations⁵¹. These collective effects, not concentrated in a single excitation, lower the single particle excitations by screening^{52,53}.

Theories for the collective excitations of π -electrons of conjugated linear chains have been presented by Araki⁵⁴ and for π -electrons on annulene molecules by Chang and Drummond.⁵⁵

3.3 Assignment of absorption structures

Since we shall present the spectra in the following sections without going into the details of the particular assignments, some general comments seem to be in order here. At least three different excitation mechanisms can contribute to the absorption cross section in the VUV which, within the MO concept, may be roughly described as:

1. Excitations of electrons from occupied to unoccupied valence orbitals with vibronic structure (normal to valence, $N \rightarrow V$, transitions). Large configuration interaction is the reason for a large spread in energy for the resulting transitions from one particular configuration, e.g. for benzene the states resulting from $\dots(a_{2u})^2(1e_{1g})^4 \rightarrow (a_{2u})^2(1e_{1g})^3(e_{2u})^1$ cover the spectral region from ~ 3 to 7.5 eV^{1,56,57}.
2. In many spectra, absorption bands can be arranged in a Rydberg series according to the Rydberg formula $E_n = E_\infty - R/(n-\delta)^2$, where E_n denotes the excitation energy of the n^{th} band, E_∞ the ionization potential, R the Rydberg constant, and n and δ the main quantum number and quantum defect respectively.^{58,59} The last is a measure for the penetration of the excited electron into the ion core.

From the analysis of Rydberg series the ionization potential (IP) towards which the series is converging may be determined. This is easy in most cases only for the lowest IP, where the determination from absorption data is more accurate than from photoelectron spectra. For higher IP's the complex absorption pattern of overlapping bands normally makes such an analysis difficult and the IP's as determined by PES are used. When all the complex absorption structures can be arranged into various Rydberg series plus their vibrational satellites one gets unambiguous information on the number of different Rydberg series converging to one particular IP. From this, even without quantitative theoretical information on the magnitude of the quantum defects

the degeneracy of the originating orbitals can be determined. The quantum defect may help for a group theoretical assignment of a series. For $\delta \approx 1$, $\delta \approx 0.5$ and $\delta \approx 0.1$ the series is probably s-, p-, or d-type respectively. The comparison of quantum defects for a homologous series of molecules may reveal trends and regularities, which help in the assignment⁵⁹. It is worth noting, that a complete analysis of Rydberg bands, as sketched above, gives information about the originating orbital (e.g. its degeneracy and symmetry) which is difficult to obtain otherwise.

If vibrational structure is resolved and compared with the absorption pattern of the deuterated molecule and with the vibrational structure in its ground state, i.e. its infrared and Raman spectra, the binding character of the originating MO can be determined.

3. Absorption structure of the kind described above is observed for energies in excess of the first IP on top of the continuous absorption due to photoionization. This large background and the overlap of different transitions makes it quite difficult to obtain a comprehensive analysis of a particular spectrum in the VUV.

3.4 Aspects of optical reflection and electron spectroscopy on organic molecular crystals

Optical reflection spectroscopy and the electron spectroscopy with fast electrons³¹⁻³³ probes for the singlet dipole excitations of the organic crystal. In both techniques, only long wavelength excitations of the crystal are involved, provided, the \underline{k} -transfer in the inelastic electron scattering is small in comparison with the extension of the Brillouin zone. Therefore, the

experiments are well described within the dielectric theory. The crystal is characterized by the dielectric tensor $\underline{\underline{\epsilon}}(\omega, \underline{k})$. No reflection experiment on organic crystals has been reported as yet, which gives conclusive evidence for spatial dispersion effects, i.e. the dependency of $\underline{\underline{\epsilon}}$ on \underline{k} . In the following it is assumed that $\underline{\underline{\epsilon}}(\omega, \underline{k})$ may be replaced by $\underline{\underline{\epsilon}}(\omega)$. For monoclinic crystals, the tensor components are evaluated by Kramers-Kronig analysis of normal incidence reflection spectra from the (001) and (010) planes, as discussed in detail in reference²⁰.

For anthracene as an example $\underline{\underline{\epsilon}}(\omega)$ may be considered as diagonal in the cartesian system xyz (see Fig. 16) which is defined by the monoclinic axis \underline{b} and the projection \underline{L} of the long molecular axis on the (010) plane. Electron spectroscopic results³⁹ and detailed reflection measurements⁶⁰ prove, that the nondiagonal elements of $\underline{\underline{\epsilon}}$ in the xyz system may be neglected in first order of approximation below the excitation energy of 10 eV.

Once the complete dielectric tensor has been evaluated, one may analyze the physical origin of all the structures, observed in the reflectance from particular crystal planes - for instance for the natural cleavage plane (001) and the electric vector perpendicular to the \underline{b} axis^{39,60}.

The long range dipole-dipole interaction of the molecules gives rise to the so-called directional dispersion of the excitons^{20,39,60}, which is a macroscopic effect. It may be either analyzed by calculating excitation energies within a lattice of interacting dipoles⁶¹ or by calculating reflectance spectra and electron energy loss spectra from the dielectric tensor^{20,39,60}.

Directional dispersion manifests itself as shown qualitatively in Fig. 6. The lower edge of the shaded area is the directional dispersion curve of the exciton with the direction of wave vector \hat{k} in a crystal with only one molecular excitation polarized in direction \hat{t} . $P(\omega, \hat{k})$ is the electron loss spectrum for energy loss $\hbar\omega$ and direction of momentum transfer \hat{k} . The height of the peaks for $P(\omega, \hat{k})$ is proportional to the magnitude of the longitudinal component of the dielectric polarization of the exciton. The shaded area shows the extension of the normal incidence reflection band due to the exciton for a given angle α_{ref} between \hat{t} and the normal of the reflecting plane^{39,60}. Its breadth, which varies from the full transverse - longitudinal splitting for $\alpha_{\text{ref}} = 90^\circ$ to zero for $\alpha_{\text{ref}} = 0^\circ$ is proportional to the transverse component of the dielectric polarization of the exciton, which has its wavevector in the direction \underline{n} .

The oscillator strength of a particular electronic dipole transition in the free molecule may be directly compared with the oscillator strength f_{exciton} of the corresponding exciton in the crystal:

$$f_{\text{exciton}} = \frac{2}{3\pi\omega_p^2} \left(\sum_{i=x,y,z} \left(\int \omega \text{Im}\epsilon_i(\omega) d\omega \right)^2 \right)^{1/2} \quad (7)$$

with $\omega_p^2 = 4\pi Ne^2/m$

Here, N is the number of molecules per unit cell, and the integral is over the exciton band. The polarization direction of the electronic molecular excitation is obtained⁶² from the distribution of the oscillator strength among the 3 tensor components.

The molecular short range interactions between nearest neighbours involve higher multipole components, e.g. Ref. 43 and 61. Their contribution to the crystal field splitting is usually small compared to the one due to dipole

dipole interaction, which causes the directional dispersion.

This macroscopic effect is minimized for pure transverse excitations. Therefore it is the Davydov splitting of the transverse excitons which contains the experimental information on the molecular short range interaction. Since the only transverse excitations of the crystal are the ones described above in connection with the evaluation of the dielectric tensor²⁰ the transverse Davydov splitting is the energy difference of exciton peak positions between $\text{Im}\epsilon_y$ and $\text{Im}\epsilon_x$ or $\text{Im}\epsilon_z$.

4. Alkanes

The electronic spectra of alkanes are of interest because transitions of the σ -electrons are not masked in these completely saturated hydrocarbons by transitions of π -electrons. Their spectra have been extensively studied during the last years for photon energies below ~ 11 eV for the gaseous^{63,64} and solid phase^{65,66}. For a review on the discussion of these spectra, in particular the question whether the observed structures are due to N-V transitions or Rydberg excitations, we refer to^{7,8}.

For photon energies up to 35 eV the absorption spectra of methane, ethane, propane and butane have been measured with synchrotron radiation (Fig. 7, 8)²⁶. For all alkanes the first two strong bands are followed by a large increase of the absorption cross section. This increase up to approximately 15 eV is not entirely structureless as was concluded from measurements with line sources. Above 16.5 eV the cross sections for all four molecules decrease smoothly to higher energies. Similar results have been obtained from electron impact spectra^{66,68-70} and conventional optical experiments (see the references given in Ref. 26).

It now seems to be widely accepted^{7,70} that almost all the observed discrete structures superimposed on the continuum absorption at higher energies are due to Rydberg type excitations, although only in very few cases more than one member of a "series" can be assigned with any certainty. We have indicated in Table 1 such tentative assignments mainly based on the interpretation of the spectra as given by Robin⁷. The problem how to identify any N-V transition underlying the Rydberg excitations still remains. For the interpretation of the vibrational bands observed for ethane, we refer to Ref. 72 and 73.

The spectra of methane, ethane and butane have been remeasured recently in the extreme VUV⁵⁰. Again synchrotron radiation served as a light source. In this experiment the absolute cross section in the range 17.5 to 69 eV were determined with a double ionization chamber. As expected from the electronic structure as determined by photoelectron spectroscopy and ESCA (e.g. Ref. 5 and 6) no new structure was detected. A similar decrease with increasing photon energy had already been observed for methane in the range 20 to 120 eV with conventional techniques⁷⁴. The hump observed at around 35 eV in Ref. 74 is not confirmed by the new experiments⁵⁰.

Structure due to transitions from the 1s electrons of the carbon K-shell at around 290 eV has been observed by Chun²⁸. This threshold region of the carbon K-absorption edge has received considerable interest recently from a theoretical point of view^{75,76}. Judging from the term values for the absorption features at 287.2 eV (weak) and 288.3 eV (strong)²⁸ relative to the carbon 1s ionization potential at 290.8 eV⁶ an assignment of the structure as being due to 1s→3s and 1s→3p Rydberg excitations seems most plausible⁷⁵. Similar experiments on related hydrocarbons, which are feasible with synchrotron radiation in this spectral range, would be very useful for a systematic comparison of Rydberg transitions, in particular their term values, originating at different shells.

Reflectance spectra from polycrystalline films from solid methane and ethane at 30 K which for the observed low reflectivities of max. 10 % resemble the absorption of the films quite accurately, are compared with the gaseous absorption for photon energies 5 to 35 eV in Fig. 8²⁶ (see also Table 1). The shapes and the positions of the bands are in good agreement with absorption spectra obtained by Lombos et al.⁶⁶ for energies up to 11 eV. The

optical constants obtained for solid methane by Daniels and Krüger⁶⁹ from electron energy loss measurements corroborated the results of the optical experiment in the whole spectral range up to 35 eV.

The positions of the first bands do not shift appreciably on solidification and the spectra from the gas and solid phase do look similar. However, a detailed understanding of these spectra from polycrystalline films is still missing. One would, for instance, expect a change in the optical spectrum for solid methane on changing its temperature, since the lattice constant shows small anomalies at 20 K and 65 K⁷⁷. Such detailed experiments still remain to be done.

5. Benzene

A thorough understanding of the electronic structure of benzene serves as the basis for an investigation of more complex organic molecules. In spite of many optical and energy loss experiments as well as photoelectron spectroscopic studies (for references see^{1,2,5,7,84}) some obvious questions and puzzles remained^{78,79}. Especially the energetic ordering of the second and third uppermost occupied MO is under discussion, as well as the assignment of the ionization potentials at 15.5 and 16.84 eV.

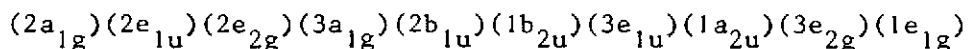
The main features of the benzene absorption in the VUV have been inferred from electron energy loss experiments^{36,80} (see Fig. 4, 5). Electron loss spectra for a number of ring compounds related to the benzene molecule have recently been obtained by Killat^{81,82}. Quite a few conclusions were derived from the electron impact spectrum measured by Lassetre et al.⁸⁰ in a detailed discussion by Johnsson and Lindholm⁸³. However, the resolution in all the electron energy loss spectra was comparatively low.

A survey of the optical absorption spectra obtained with synchrotron radiation^{84,85} is shown in Fig. 9 covering the photon energy range 5 to 35 eV. Following the intense $\pi-\pi^*$ transition at about 6.9 eV, a broad and continuous absorption with a maximum at about 17.8 eV is observed. Here the cross section reaches values of about 150 Mb (see Ref. 86 and Fig. 4). It decreases smoothly for higher photon energies. The main features of the absorption cross section except, for additional details revealed by the synchrotron light experiment, are in good agreement with those of Ref. 86-88.

The spectral range up to 9.2 eV has been extensively discussed in Ref. 1. Ab initio SCF MO and CI calculations have been carried out for benzene in

different approximations^{56,57,89} and the calculated transition energies have been compared with experiment. Unfortunately the assignments can be made with confidence only for excitation energies below ~ 8 eV. Above this energy the spectrum is heavily overlapping and, although the $\sigma-\pi^*$ and the $\sigma-\sigma^*$ transitions must fall in this energy region, little else can be said.

In Fig. 10 the spectral region between 10 and 15 eV is shown on an expanded scale⁸⁵. For the detailed discussion of the complex absorption structure we refer to Ref. 84 and 85. The result of our assignment is indicated in Fig. 10, where the absorption bands are assigned to Rydberg series converging to the ionization potentials at 11.49 and 11.71 eV. Our analysis of the spectrum implies the following ordering of the occupied valence MO's with decreasing binding energy:



This ordering is in accordance with most of the recent MO calculations, e.g. Ref. 90, 91. Thus the second ionization potential at 11.49 eV corresponds to the uppermost $\sigma-3e_{2g}$ orbital and only p-type series are expected. This implies that the third ionization potential is $1a_{2u}$ (π -type) and only one s-type series should be observed. This series is seen in Fig. 10 leading to the ionization potential at 11.71 eV.

These conclusions have not been obtained from the analysis of the benzene spectrum alone. Recent measurements on perdeutero-benzene and fluorinated benzenes and pyridene in the same spectral region⁸⁵ gave further support for the assignments. In particular, the weak s-type series, which could not be found in earlier absorption spectra because of the lower experimental accuracy, can be assigned clearly in the spectra from C_6H_5F and C_6F_6 where

it is not overlapping the p-type series. Furthermore this assignment is in accordance with the results from photoelectron spectra^{5,92}. It requires, however, placement of the second IP at 11.71 eV rather than ~ 12.2 eV, the value adopted in most interpretations. Thus the unassigned maximum at 11.71 eV in the photoelectron spectrum of Åsbrink et al.⁹³ which show the best resolution so far obtained, gets a natural explanation.

Recently there was some debate on the correct assignment of the IP at around 15.40 and 16.85 eV⁷⁸. The absorption spectra in the range 14 to 18 eV for benzene and perdeuterobenzene are shown in Fig. 11⁸⁵. In both spectra a p-type series leading to an IP at 16.84 and 16.85 eV respectively can be assigned (see also Ref. 84). Thus the originating orbital must be $3a_{1g}$. This result agrees with the conclusion drawn from recent high resolution ESCA work on benzene⁹⁵.

The investigation of the excited states of liquid and solid benzene in the VUV is still in its beginning. Williams et al.⁹⁶, Sowers et al.⁹⁷, and Inagaki⁹⁸ reported on the optical properties of liquid benzene up to ~ 10 eV. For photon energies below 8 eV the excited states of solid polycrystalline benzene have been studied by optical spectroscopy^{99,100}. Only recently studies of the 2000 Å system of benzene single crystals became available^{101,102}. For higher energies, polycrystalline benzene films have been studied in electron energy loss^{81,103} and reflectance experiments (see Fig. 12)¹⁷. The data obtained from the energy loss function⁸¹ are in good agreement with the reflectance measurements. However, a detailed understanding of the structured reflectance bands or loss function is still missing.

6. Naphthalene

For the naphthalene ($C_{10}H_8$) molecule with a total of 48 valence electrons the problem of overlapping bands is even worse. Its absorption spectrum in the visible and near UV has been discussed and compared to MO-calculations (for references see 104). Electron loss spectra for excitation energies up to 30 eV revealed intense absorption at higher energies with a maximum at about 17.5 eV³⁶. Recently Huebner et al.¹⁰⁵ reported on loss spectra with 100 eV incident electrons and increased resolution (0.04 eV compared to ~ 0.7 eV) from which a summed oscillator strength below 8.12 eV for $f=2.25$ was deduced.

The results from optical absorption experiments in the range 5 to 30 eV with comparatively high resolution have been discussed in detail in Ref. 104. From comparison with photoelectron spectra, e.g. Ref. 5, and MO assignments based on the calculations of Ref. 106, tentative assignments for a number of Rydberg series could be given.

One interesting point of the discussion is the possibility that Fano-Beutler resonances¹⁰⁷ occur. Some of the absorption profiles observed in the naphthalene vapour spectrum at around 7.5 eV (see Fig. 13) have been ascribed to such antiresonances^{108,109} caused by interference of energetically degenerate Rydberg states with the quasi continuous $\pi-\pi^*$ band. Spectra with improved resolution would clarify this point.

7. Anthracene

In organic solid state physics anthracene plays an important role both for the investigation of semiconducting properties and for the study of molecular excitons, e.g.^{61,110}. Our work is concerned with the investigation of the electronic transitions of the molecule¹¹¹ and the excitons they give rise to in the crystal^{39,60,62}. In view of the need to use polarized light for the investigation of the optical anisotropy of single crystals, the spectral range above the first singlet exciton (~ 3.1 eV) is not easily accessible with conventional spectroscopic techniques.

The starting point of our considerations are the electronic transitions of the free molecule in the ultraviolet, about which only little was known. Relevant results on solid anthracene will be presented in the following section.

7.1 Absorption spectrum of the anthracene molecule

The optical absorption spectrum for energies from 5 to 8.5 eV¹¹¹ is shown in Fig. 14. It differs quite markedly from those spectra reported earlier for parts of this spectral range^{112,113}. These differences are discussed in detail in Ref. 111 and are thought to be mainly due to some radiation or clogging effects on the LiF windows in the earlier experiments. Compared with the spectrum obtained by Kitagawa¹¹⁴, there is fair agreement for photon energies up to ~ 7.5 eV, which is the upper limit of the older experiment. Our interpretation of the sharp absorption bands (see below) differs, however, from that proposed in Ref. 114. The results obtained by Clark¹¹⁵ are in excellent agreement with our spectrum.

The sharp maxima at 6.26, 6.43 and 6.53 eV and the bands superimposed on the broad 6.9 eV band (Fig. 14) belong to Rydberg series. Angus and Morris¹¹³ assigned 5 series. From these they deduced a value of 7.15 eV for the first ionization potential. We are unable to confirm this assignment on the basis of our spectra. Recent photoelectron spectra show that the first four ionization potentials associated with the removal of the outer π -electrons fall at 7.47 eV ($2b_{2g}$), 8.57 eV ($2b_{1g}$), 9.23 eV ($1a_u$) and 10.26 eV ($2b_{3u}$)^{116,117}. The notation is in accordance with the convention as given in Ref. 118. As for benzene and naphthalene, the presence of Rydberg series with higher ionization potentials as well as the occurrence of additional vibrational bands makes an unequivocal assignment difficult. In Fig. 14 two series accompanied by vibrational bands with quantum defects $\delta=0.64$ and $\delta=0.2$ which account for several of the most prominent bands are indicated. They both lead to the first ionization potential at 7.47 eV.

Some information about the transitions of the free molecule at higher excitation energies can be obtained from studies of electron energy loss spectra^{36,38}. Although these experiments (Fig. 15) were limited by a comparatively low resolution one obtains from Fig. 15 a good general overview on the spectrum above the LiF cut off. The most prominent absorption bands are a broad shoulder at 11.3 eV and a maximum of the cross section at about 17 eV.

7.2 Dielectric properties and singlet excitons of solid anthracene

The dielectric tensor elements within the x,y,z-system (see Fig. 16) at room temperature are displayed in Fig. 17⁶⁰. Experimental details and the accuracy of the Kramers-Kronig analysis of the reflection spectra have been discussed in Ref. 62. Reflection spectra from the $(20\bar{1})$ and $(\bar{1}10)$ -planes and a set of artificially cut planes containing the (010) axis have been reported by Clark and coworkers¹¹⁹⁻¹²².

As mentioned in section 3.4 the distribution of the oscillator strength of an exciton over the directions x,y,z allows the assignment of the corresponding molecular excitations to (i) the transitions ${}^1B_{2u} \leftarrow {}^1A_{1g}$, where the polarization vector lies along the long axis of the molecule, (ii) to transitions ${}^1B_{1u} \leftarrow {}^1A_{1g}$, where the polarization vector lies along the short axis of the molecule and (iii) to transitions ${}^1B_{3u} \leftarrow {}^1A_{1g}$ where it lies perpendicular to the molecular plane. A compilation of the exciton energies of anthracene in the single crystal, the vapour phase, and in solution is presented in Table 2.

A comparison of the oscillator strength of the long axis polarized ${}^1B_{2u}$ transition at 4 to 5.5 eV is given in Table 3. Following the usual practice, Lorentz-Lorenz corrections have been neglected. In Fig. 18 n_{eff} is shown for the three tensor components, as calculated from the optical constants in Fig. 17 using the relation²⁰: (spectra for $\underline{E} \parallel \underline{M}$ and $\underline{E} \perp \underline{L}$ are, within the experimental accuracy the same)

$$n_{\text{eff}}(\omega) = \frac{m}{2\pi^2 N e^2} \int_0^\omega \text{Im}\epsilon(\omega') \omega' d\omega' \quad (8)$$

As allows from the comparison with equation 7 in section 3.4, n_{eff} is closely related to the oscillator strength of the molecular transitions.

A comparison of the Davydov splitting of the most intense exciton at about 4.56 eV with theoretical calculations of Philpott¹²⁹ allows a check on the microscopic interaction of molecules, as discussed in section 3.4. The experimental Davydov splitting of this exciton taken as the difference in ϵ_2 peak positions from the (010) and (001) planes is -0.02 ± 0.03 eV. When this splitting is calculated within the dipole approximation¹²⁹, the result is 0.31 eV. The agreement becomes excellent when higher multipole terms calculated from the resonance interaction of Pariser Parr molecular wavefunctions are included. Philpott¹²⁹ rescaled the corresponding lattice sums of Silbey et al.¹³⁰ and

found a Davydov splitting of 0.01 eV.

The reflection spectra from planes parallel to the \underline{b} -axis and the electric vector $\perp \underline{b}$ have been measured by Hymowitz and Clark¹²² in order to probe for the directional dispersion of the strong exciton (see Fig. 19). There is a rough correspondence to the simple case discussed in section 3.4 in connection with Fig. 6. All the structure is well reproduced without any fitting by calculating the reflection spectra with the help of the dielectric tensor components ϵ_x, ϵ_z . In this way, also the origin of the double structure in the reflection from the (001) plane and $\underline{E} \perp \underline{b}$ ($\alpha=29.5^\circ$ in Fig. 19) may be explained⁶⁰. The lower peak at about 5.67 eV originates from an exciton of a molecular ${}^1B_{1u} \leftarrow {}^1A_{1g}$ transition, the upper near 6.08 from the long axis polarized exciton of the molecular ${}^1B_{2u} \leftarrow {}^1A_{1g}$ transition (see Table 2).

Information on the exciton structure of organic solids is also obtained from electron loss spectroscopy. Venghaus¹³¹ evaluated the energy loss function $\text{Im}(\epsilon^{-1})$ for the three directions x,y,z for anthracene. In Fig. 20 these data are compared to the loss function as calculated from the optical data from Fig. 17. The better resolution of the optical spectra is obvious.

Kunstreich and Otto³⁹ probed for the directional dispersion of the excitons, which may be measured for one thin crystalline flake rather than on many artificially prepared faces (Fig. 19). In Fig. 21 characteristic energy loss spectra for various directions of \underline{k} are displayed. The directional dispersion of the excitons, as given by the peak positions in these spectra is plotted in Fig. 22. For comparison see the simple model as described by Fig. 6. For the excitons with excitation energies below 10 eV, which have been discussed above (Table 2), the directional dispersion is symmetric with respect to the

directions x and z. Above 10 eV this symmetry no longer exists. This indicates axial dispersion of the dielectric tensor²⁰.

8. Aromatic hydrocarbons and related compounds

8.1 Higher aromatic hydrocarbons

Energy loss spectra for gaseous polyacenes up to tetracene, for phenanthrene, chrysene, pyrene and coronene³⁶ as well as for triphenylene and perylene³⁷ have been obtained in our laboratory. For these molecules, comparison with optical absorption measurements, e.g. Ref. 132 and MO-calculations, e.g. Ref. 133, 134, lead to an assignment of several losses as being due to $\pi\text{-}\pi^*$ one electron transitions. In Fig. 23 calculated excitation energies for the ${}^1B_{1u}$ and ${}^1B_{2u}$ $\pi\text{-}\pi^*$ transition in the polyacene molecules are compared with the measured energy losses. The interpretation of loss maxima at higher excitation energies, where a broad absorption with maximum cross section between 15 and 18 eV is observed for all molecules, is still tentative. In this energy range, not yet covered by optical measurements, a large number of $\sigma\text{-}\pi^*$ and $\sigma\text{-}\sigma^*$ N-V transitions is expected, as well as a manifold of Rydberg transitions. Recently photoelectron spectra have become available for a number of these molecules^{116,135,136}. Although they are helpful for labeling the ionization potentials of the weakly bound π -orbitals, even photoelectron spectra do not permit a decomposition of the broad bands corresponding to σ -electron binding energies in the range 10 - 30 eV.

For polycrystalline films energy loss spectra have been obtained for a number of hydrocarbons by Jäger¹³⁷. The loss spectrum for such films of hexabenzocoronene has been measured by Gutfreund and Little⁵¹. The dielectric tensor elements for phenanthrene ($C_{14}H_{10}$), chrysene ($C_{18}H_{12}$)¹³⁸ and pyrene ($C_{16}H_{10}$)¹³⁹ have been derived from electron energy loss experiments in the range 0 to 40 eV on single crystals. The results obtained were discussed in comparison with excited molecular states as regards excitation energy and polarization.

For a synopsis of the main results from optical and electron energy loss measurements on the gaseous and solid phase of aromatic hydrocarbons we refer to table 4. In addition values taken from solution spectra are given for comparison. Only values for maxima of the most prominent $\pi-\pi^*$ transitions where an assignment is not controversial, are cited. For details of the assignments the original papers should be consulted. These data make possible quantitative statements about the interesting problem of gas to solid shifts, i.e. the differences in the excitation energies between vapour phase and the solid for those excitations, where a common origin is obvious.

In those cases where a comparison between the optical and energy loss measurements for the vapour phase is possible (benzene, naphthalene and anthracene) there is an excellent agreement as regards the peak positions. For all substances there occurs an appreciable vapour to liquid shift, in some cases of the order of 0.4 eV.

Whereas in the case of the electron energy loss experiments it is only possible to give a qualitative measure for the gas to solid shifts (in the order of 0.3 eV) due to the comparatively poorer resolution for both the vapour and the crystal measurements, there is more detailed information available from the optical experiments, which in addition show vibrational fine structure. However, a definite determination of peak positions and assignment has to be made with caution, since there might occur strong shifts and splittings due to the directional dispersion as for instance for the case $\underline{E} \parallel \underline{a}$ on (001) for anthracene⁶⁰ (see section 7.2).

It is hoped that such data as compiled in this table is of some help for an understanding of the gas to solid shifts, which are obviously not "disagreements" in experimental results as stated in Ref. 139. A satisfactory

quantitative theoretical account of these shifts, is presently still missing.

8.2 Related experiments on other organic compounds

The number of optical and energy loss experiments on more complicated organic compounds for excitation energies in the VUV is steadily increasing. The energy loss spectrum for the sandwich type molecule ferrocene³⁷ is shown as an example in Fig. 24 and compared to the optical absorption spectrum¹⁴³. Except for the strong absorption at about 6.6 eV which can be assigned to a $\pi-\pi^* \quad {}^1E_{1u} \leftarrow {}^1A_{1g}$ transition (point group D_{5d} ¹⁴⁴) the absorption structures at higher energies are as yet unassigned.

Similar experiments as for the single crystals of aromatic hydrocarbons were done by Venghaus in order to determine the dielectric tensor for monoclinic crystals of p-terphenyl ($C_{18}H_{16}$) and orthorhombic crystals of fluoren ($C_{13}H_{10}$)¹⁴⁵.

Okabe¹⁴⁶ recently reported on energy loss spectra for polycrystalline films of β -carotene, diphenylpolyenes and paraffins applying 40 keV electrons, from which spectra of the dielectric functions via a Kramers-Kronig analysis could be derived.

A group of important biological materials, the nucleic acid bases adenine, thymine and uracil has been studied by Isaacson^{147,148} for outer and inner shell excitations by means of electron loss measurements.

In a later experiment it was tried to obtain optical constants from biological compounds by reflectance measurements for photon energies 5 to 25 eV with a synchrotron light source¹⁴⁹. However, due to the diffuse reflectance from most samples only the measurements on cytosine have been successful. They yielded roughly the same results as the energy loss experiments, with more sharply defined peaks and some additional structure above 10 eV.

This list of experiments on compounds of biological importance is by far not complete. The few examples just illustrate the experimental problems and the present understanding of the higher electronic states of such compounds. Once the difficulties in sample preparation can be overcome the next future will bring more results and information on similar systems.

9. Final remarks

As mentioned in the introduction, only some experimental results have been described, and often a more complete analysis would have been desirable. In this regard several comments about our present understanding and the necessity of future studies on the excited states of organic molecules and molecular crystals seem to be in place here.

The VUV spectra above ~ 7 eV of larger organic compounds are often complex and diffuse, since they are composed of a large number of overlapping valence shell and Rydberg transitions. Nevertheless it is felt, that future efforts will help to obtain more quantitative results. For instance, the Rydberg nature of several absorption bands links optical VUV and photoelectron spectroscopy closely, and work in one area will stimulate progress in the other.

The determination of absolute cross sections and f -values, the analysis of absorption band shapes and vibrational fine structure in spectra with improved resolution seems rewarding, and has hardly been attempted. The possibility of finding collective modes in electron energy loss spectra with large momentum transfer has already been mentioned.

Additionally one might hope to have the chance to compare the experimental results with improved MO-calculations. Such a comparison is not yet possible on a large scale due to the absence of accurate calculations for molecules with a total of more than approximately 30 valence electrons. However, several semiempirical (e.g. Ref. 150) and ab initio (e.g. Ref. 106) calculations are in progress, which go beyond this limit.

Optical and electron-impact spectroscopy covering the whole range of valence electron excitations will be stimulated by recent developments in photochemistry, where fragmentation and reaction processes are being studied via mass-spectro-

scopy, fluorescence, and its time dependence (e.g. Ref. 8). Thus a chemistry of molecules in their excited states seems possible.

As far as the comparison of vapour and solid state spectra is concerned, valuable future contributions along the lines indicated above are expected from both optical and energy loss spectroscopy. In addition, interesting new phenomena, such as the occurrence of surface excitons^{†51,152} and an investigation of dynamical properties of excitons with higher excitation energies in the VUV will be investigated. Generally such studies will be stimulated by the growing interest in organic solid state phenomena.

Acknowledgment

We would like to thank our colleagues from the synchrotron radiation group at DESY and from Munich University for their support. We are especially indebted to J. Huber, K.L. Kliewer, S. Kunstreich, K. Radler, V. Saile, N. Schwentner, and M. Skibowski for their cooperation in several of the experiments described above and for the fruitful discussions we enjoyed with them.

Thanks are also due to L. Åsbrink, R. Boschi, L.B. Clark, U. Killat, E. Lassetre, E. Lindholm, M.R. Philpott, W.C. Price, and H. Venghaus for generously making available to us results of experiments and calculations prior to publication. Stimulating discussions with them as well as with M.B. Robin and J. Dow, are gratefully acknowledged.

References

1. G. Herzberg, Molecular Spectra and Molecular Structure, Vol. 3, van Nostrand, N.Y. (1966)
2. H.H. Jaffé and M. Orchin, Theory and Applications of Ultraviolet Spectroscopy, Wiley, N.Y. (1962)
3. J.N. Murrell, Elektronenspektren organischer Moleküle, Bibliogr. Inst., Mannheim (1967)
4. R.L. Platzman, Rad.Res. 17, 419 (1962)
5. D.W. Turner, C. Baker and C.R. Brundle, Molecular Photoelectron Spectroscopy, A Handbook of the 584 Å Spectra, J. Wiley, New York (1970)
6. K. Siegbahn, C. Nordling, G. Johansson, J. Hedman, P.F. Hedén, K. Hamrin, U. Gelius, T. Bergmark, L.O. Werme, R. Manne and Y. Baer, ESCA Applied to Free Molecules, North Holland, Amsterdam (1969)
7. M.B. Robin, Higher Electronic States of Polyatomic Molecules Vol. 1, Vol. 2, Acad.Press, N.Y. (1974) in press
8. Chemical Spectroscopy and Photochemistry in the Vacuum-Ultraviolet, edited by C. Sandorfy, P.J. Ausloos and M.B. Robin, D. Reidel Publ. Comp. Dordrecht/Boston (1974)
9. A.A. Sokolov and J.M. Ternov, Synchrotron Radiation, Acad. Verlag Berlin (1968)
10. J.A.R. Samson, Techniques of Vacuum Ultraviolet Spectroscopy, J. Wiley, N.Y. (1967)
11. A.N. Zaidel and E.Y.A. Schreider, Vacuum Ultraviolet Spectroscopy, translated from the Russian, Ann Arbor-Humphrey, Ann Arbor (1970)
12. R. Haensel and C. Kunz, Z.Angew.Phys. 23, 276 (1967)
13. R.P. Godwin, Springer Tracts in Modern Physics 51, 1 (1969)
14. K. Codling, Rep.Prog.Phys. 36, 541 (1973)
15. F.C. Brown, in Solid State Physics ed. by H. Ehrenreich, F. Seitz and D. Turnbull, in press

16. E.E. Koch and C. Kunz, Synchrotronstrahlung bei DESY, ein Handbuch für Benutzer, DESY (1974)
17. E.E. Koch, Thesis, München (1973)
18. M. Skibowski and W. Steinmann, J.Opt.Soc.Am. 57, 112 (1967)
19. U. Backhaus, Diplomarbeit, Hamburg (1973)
20. E.E. Koch, A. Otto, and K.L. Kliewer, Chem.Phys. 3, 362 (1974)
21. R. Haensel, G. Keitel, E.E. Koch, M. Skibowski, and P. Schreiber, Phys.Rev.Letters 23, 1160 (1969)
22. R. Haensel, G. Keitel, E.E. Koch, M. Skibowski, and P. Schreiber, Optics Commun. 2, 59 (1970)
23. R. Haensel, G. Keitel, E.E. Koch, N. Kosuch, and M. Skibowski, Phys.Rev.Letters 25, 1281 (1970)
24. R. Haensel, E.E. Koch, N. Kosuch, U. Nielsen, and M. Skibowski, Chem.Phys.Letters, 9, 548 (1971)
25. E.E. Koch and M. Skibowski, Chem.Phys.Letters 14, 37 (1972)
26. E.E. Koch and M. Skibowski, Chem.Phys.Letters 9, 429 (1971)
27. E.E. Koch, in Ref. 8, p. 559
28. H.K. Chun, Phys. Letters 30A, 445 (1969)
29. E.N. Lassette and A. Skerbele, Inelastic Electron Scattering in: Experimental Methods of Molecular Physics, in press
30. E.N. Lassette, in Ref. 8, p. 43 and references therein
31. H. Raether, Springer Tracts in Modern Physics 38, 84 (1965)
32. J. Geiger, Elektronen und Festkörper, Sammlung Vieweg Bd. 128 Vieweg, Braunschweig (1968)
33. J. Daniels, C.v. Festenberg, H. Raether and K. Zeppenfeld, Springer Tracts in Modern Physics 54, 77 (1970)
34. S. Kunstreich, Diplomarbeit, München, 1968
35. S. Kunstreich and A. Otto, Opt.Comm. 1, 45 (1969)

36. E.E. Koch and A. Otto, *Opt.Comm.* 1, 47 (1969)
37. E.E. Koch and A. Otto, *Chem.Phys.Letters* 6, 15 (1970)
38. E.E. Koch, S. Kunstreich and A. Otto, *Opt.Comm.* 2, 365 (1971)
39. S. Kunstreich and A. Otto, *Chem.Phys.* 3, 384 (1974)
40. H. Bethe, *Ann.Phys.* 5, 325 (1930)
41. H.S.W. Massey and E.H.S. Burhop, *Electronic and Ionic Impact Phenomena*, Vol. 1, Oxford (1969)
42. U. Fano and J.W. Cooper, *Rev.Mod.Phys.* 40, 441 (1968)
43. D.P. Craig and S.H. Walmsley, in: *Physics and Chemistry of the Organic Solid State*, Vol. 1, p. 585, edited by D. Fox, H.M. Labes, and A. Weissberger J. Wiley, New York (1963) and references therein
44. H. Guffreund and W.A. Little, *Chem.Phys.Letters* 2, 589 (1968)
45. J. Höhberger, A. Otto, and E. Petri, submitted to *Phys.Rev.Letters*
46. O. Sinanoglu and K.A. Brueckner, *Three Approaches to Electron Correlation in Atoms*, Yale Univ. Press (1970)
47. M.Ya. Amusia, N.A. Cherepkov, and L.V. Chernyshev, *Physics Letters* 31A, 553 (1970)
48. G. Wendin, *J.Phys. B* 6, 42 (1973) and references therein
49. A. Herzenberg, D. Sherrington and M. Süveges, *Proc.Phys.Soc.* 84, 465 (1964)
50. L.C. Lee, R.W. Carlson, D.L. Judge and M. Ogawa, *J.Quant.Spectr. Radiat. Transfer* 13, 1023 (1973)
51. H. Gutfreund and W.A. Little, *J.Chem.Phys.* 50, 4478 (1969)
52. W.A. Little, *J.Chem.Physics* 49, 420 (1968)
53. H. Gutfreund, and W.A. Little, *J.Chem.Phys.* 50, 4468 (1969)
54. G. Araki, *Progr.Theor.Phys., Suppl* 40, 106 (1967)
55. J.D.B. Chang and J.E. Drummond, *J.Chem.Phys.* 52, 4533 (1970)
56. S.D. Peyerimhoff and R.J. Buenker, *Theoret.Chim. Acta (Berl)* 19, 1 (1970)
57. P.J. Hay and J. Shavitt, *Chem.Phys.Letters* 22, 33 (1973)

58. A.B.F. Duncan, Rydberg Series in Atoms and Molecules, Academic Press, New York (1971)
59. see also: M.B. Robin, in Ref. 8 and references therein
60. E.E. Koch and A. Otto, Chem.Phys. 3, 370 (1974)
61. M.R. Philpott, Some modern Aspects of Exciton Theory, in: Advances in Chem.Phys. 23, 227 (1973) and references therein
62. E.E. Koch and A. Otto, phys.stat.sol. (b) 51, 69 (1972)
63. B.A. Lombos, P. Sauvageau, and C. Sandorfy, J.Mol.Spectr. 24, 253 (1967)
64. J.W. Raymond and W.T. Simpson, J.Chem.Phys. 47, 430 (1967)
65. K. Dressler and O. Schnepf, J.Chem.Phys. 33, 270 A (1960)
66. B.A. Lombos, P. Sauvageau and C. Sandorfy, Chem.Phys. Letters 1, 382 (1967)
67. E.N. Lassette, A. Skerbele, and M.A. Dillon, J.Chem.Phys. 49, 2382 (1968)
68. H. Gutfreund and W.A. Little, Phys.Rev. 183, 68 (1969)
69. J. Daniels and P. Krüger, phys.stat.sol. (b) 43, 659 (1971)
70. W.R. Harshbarger and E.N. Lassette, J.Chem.Phys. 58, 1505 (1973)
71. R.J. Schoen, J.Chem.Phys. 37, 2032 (1962)
72. E.F. Pearson and K.K. Innes, J.Mol.Spectr. 30, 232 (1969)
73. C. Sandorfy in Ref. 8 p. 177
74. L. De Reilhac, N. Damany-Aston and J. Romand, Spectrochim. Acta 25A, 19 (1969)
75. P.S. Bagus, M. Krauss and R.E. LaVilla, Chem.Phys. Letters 23, 13 (1973)
76. P.W. Deutsch and A.B. Kunz, J.Chem.Phys. 59, 1155 (1973)
77. S.C. Greer and L. Meyer, Z. Naturf. 27, 198 (1969)
78. A.W. Potts, W.C. Price, D.G. Streets and T.A. Williams, Farad. Disc. 54, 168 (1973)
79. E. Lindholm, discussion following Ref. 78
80. E.N. Lassette, A. Skerbele, M.A. Dillon, and K.J. Ross, J.Chem.Phys. 48, 5066 (1968)
81. U. Killat, Z. Phys. 263, 83 (1973)

82. U. Killat, Thesis, Hamburg (1973)
83. B.Ö. Jonsson and E. Lindholm, Arkiv Fysik 39, 65 (1969)
84. E.E. Koch and A. Otto, Chem.Phys. Letters 12, 476 (1972)
85. E.E. Koch, A. Otto, N. Schwentner, and V. Saile, to be published
86. M. Yoshino, J. Takeuchi, and H. Suzuki, J.Phys.Soc.Jap. 34, 1039 (1973)
87. S.M. Bunch, C.R. Cook, M. Ogawa, and A.F. Ehler, J.Chem.Phys. 28, 740 (1958)
88. J.C. Person, J.Chem.Phys. 43, 2553 (1965)
89. R.M. Stevens, E. Switkes, E.A. Laws, and W.N. Lipscomb, J.Am.Chem.Soc. 93, 2603 (1971)
90. R.E. Christoffersen, D.W. Genson, and G.M. Maggirra, J.Chem.Phys. 54, 239 (1971) and references therein
91. W.C. Ermler and C.W. Kern, J.Chem.Phys. 58, 3458 (1973)
92. T.A. Carlson and C.P. Anderson, Chem.Phys. Letters 10, 561 (1971)
93. L. Åsbrink, E. Lindholm, O. Edquist, Chem.Phys. Letters 5, 609 (1970)
94. M.F.A. El-Sayed, M. Kasha and Y. Tanaka, J.Chem.Phys. 34, 334 (1961)
95. U. Gelius, E. Basilier, S. Svensson, T. Bergmark, and K. Siegbahn, J.Electr.Spectr. 2, 405 (1974)
96. M.W. Williams, R.A. McRae, R.N. Hamm, and E.T. Arakawa, Phys.Rev.Letters 22, 1088, 1969
97. B.L. Sowers, E.T. Arakawa, and R.D. Birkhoff, J.Chem.Phys. 54, 2319 (1971)
98. T. Inagaki, J.Chem.Phys. 57, 2526 (1972)
99. V.L. Broude, Sov.Phys.-Ups. 4, 584 (1962)
100. M. Brith, R. Lubart and I.T. Steinberger, J.Chem.Phys. 54, 5104 (1971)
101. A. Brillante, C. Taliani and C. Zauli, Mol.Phys. 25, 1263 (1973)
102. D.A. Bird and J.H. Callomon, Mol.Phys. (1973)
103. A. Otto and M.J. Lynch, Aust. J. Phys. 23, 609 (1970)
104. E.E. Koch, A. Otto and K. Radler, Chem.Phys.Letters 16, 131 (1972)
105. R.H. Huebner, S.R. Mielczarek, and C.E. Kuyatt, Chem.Phys.Letters 16, 464 (1972)

106. R.J. Buenker and S.D. Peyerimhoff, Chem.Phys. Letters 3, 37 (1969)
107. U. Fano, Nuovo Cimento 12, 156 (1935), Phys.Rev. 124, 1866 (1961)
108. J. Jortner and G.C. Morris, J.Chem.Phys. 51, 3589 (1969)
109. R. Scheps, D. Florida, and S.A. Rice, J.Chem.Phys. 56, 295 (1972)
110. A.S. Davydov, Theory of Molecular Excitons, Plenum, New York (1971)
111. E.E. Koch, A. Otto, and K. Radler, Chem.Phys. Letters 21, 501 (1973)
112. L.E. Lyons and G.C. Morris, J.Mol.Spectr. 4, 480 (1960)
113. J.A. Angus and G.C. Morris, J.Mol.Spectr. 21, 310 (1966)
114. T. Kitagawa, J.Mol.Spectr. 26, 1 (1968)
115. L.B. Clark, private communication
116. R. Boschi, J.N. Murrel and W. Schmidt, Disc. Farad. Soc. 54, 116 (1973)
117. D.G. Streets and T.A. Williams, J.Electr.Spectr. 3, 71 (1974)
118. J.Chem.Phys. 23, 1197 (1955)
119. L.B. Clark and M.R. Philpott, J.Chem.Phys. 53, 3790 (1970)
120. L.B. Clark, J.Chem.Phys. 51, 5719 (1969)
121. L.B. Clark, J.Chem.Phys. 53, 4092 (1970)
122. V. Hymowitz and L.B. Clark, private communication
123. H.B. Klevens and J.R. Platt, J.Chem.Phys. 17, 470 (1949)
124. J. Ferguson, L.W. Peeves, and W.G. Schneider, Can.J.Chem. 35, 1117 (1957)
125. J. Ferguson, new results as cited in Ref. 112
126. L.E. Lyons and G.C. Morris, J.Chem.Soc. 1551 (1959)
127. Friedel and Orchin, Ultraviolet Spectra of Aromatic Compounds, Wiley (1951)
128. UV-Atlas Organischer Verbindungen, Butherworth, Verlag Chemie (1966)
129. M.R. Philpott, Chem.Phys. Letters 17, 57 (1972)
130. R. Silbey, J. Jortner, and S.A. Rice, J.Chem.Phys. 42, 1515 (1965)
131. H. Venghaus, Z. Phys. 239, 289 (1970)
132. R. Pariser, J.Chem.Phys. 24, 250 (1956)
133. N.S. Ham and K. Ruedenberg, J.Chem.Phys. 25, 13 (1956)
134. O.W. Adams and R.L. Miller, J.Am.Chem.Soc. 88, 404 (1966)

135. R. Boschi and W. Schmidt, *Tetrahedron Letters* 25, 2577 (1972)
136. R. Boschi, private communication
137. J. Jäger, *Ann. Phys.* 22, 147 (1969)
138. H. Venghaus, *J. Chem. Phys.* 57, 3478 (1972)
139. H. Venghaus, *phys. stat. sol. (b)* 54, 671 (1972)
140. E. Pantos and T.D.S. Hamilton, *Chem. Phys. Letters* 17, 588 (1972)
141. J. Tanaka, *Bull. Chem. Soc. Jap.* 38, 86 (1965)
142. J.P. Byrne and J.G. Ross, *Can. J. Chem.* 43, 3253 (1965)
143. D.R. Scott and R.S. Becker, *J. Chem. Phys.* 35, 516 (1961)
144. J.D. Dunitz, L.E. Orgel and A. Rich, *Acta Cryst.* 9, 373 (1961)
145. H. Venghaus, Thesis, Hamburg 1973
146. T. Okabe, *J. Phys. Soc. Jap.* 35, 1496 (1973)
147. M. Isaacson, *J. Chem. Phys.* 56, 1803 (1972)
148. M. Isaacson, *J. Chem. Phys.* 56, 1813 (1972)
149. D.E. Johnson and M. Isaacson, *Opt. Comm.* 8, 406 (1973)
150. L. Åsbrink, C. Fridh, and E. Lindholm, in Ref. 8, p. 247
151. e.g. V.J. Sugakov, *Sov. Phys. Solid State* 14, 1711 (1973)
152. J. Huber, E.E. Koch, and A. Otto, in preparation

Table 1: Excitation energies in eV for gaseous and solid alkanes and some tentative assignments (Ref.7)

Sh: shoulder, a: Ref. 26, b: Ref. 66, c: E.E. Koch, unpublished

Table 2: Position of maxima in the absorption spectrum (in eV) of the anthracene molecule, of anthracene in n-heptane solution and of ϵ_2^- and reflection spectra from anthracene single crystals for various directions of polarization

Sh: shoulder, B_{1u} corresponds to short, B_{2u} to long axis polarized transitions, a: Ref. 111, b: Ref. 38, c: Ref. 123, d: Ref. 62, e: Ref. 119, f: Ref. 60

Table 3: Oscillator strength of the ${}^1B_{2u}$ long axis polarized transition in anthracene at 4 to 5.5 eV

a: Ref. 124, b: Ref. 125, c: Ref. 112, d: Ref. 114, e: Ref. 123, f: Ref. 126, g: Ref. 127, h: Ref. 128, i: taken from Fig. 19

Table 4: Excitation energies in eV for some aromatic hydrocarbons in the vapour phase, in solution and in solid phase. For details see text.

a: Ref. 36,38, b: Ref. 84, c: Ref. 104,111, d: Ref. 98, e: Ref. 123, f: Ref. 140, g: Ref. 100, h: Ref. 62, i: Ref. 141, j: Ref. 131, k: Ref. 138, l: Ref. 139, m: Ref. 81, n: Ref. 142.

Table 1

Methane		Ethane		Propane		Butane
Symmetry: T_d		D_{3h}, D_{3d}		C_{2v}		C_{2h}
vapour(a)	solid(a)	vapour(a)	solid(a)	vapour(a)	solid	vapour(a)
9.7	$1t_2 \rightarrow 3s$	9.6	9.6	7.93	$2b_2 \rightarrow 3s$	8.65
			$\left\{ \begin{array}{l} 1e_g \rightarrow 3p \\ 3a_{1g} \rightarrow 3p \end{array} \right.$	8.85	$2b_2 \rightarrow 3p$	
					$4a_1 \rightarrow 3s$	9.4(b)
10.4	$1t_2 \rightarrow 3s$	11.0sh		9.65	$4a_1 \rightarrow 3p$	9.8(b)
			$10.7 \{ \rightarrow 4p$			10.3(b)
11.7	$1t_2 \rightarrow 4s$	11.8		11.0	$1a_2 \rightarrow 3p$	11.2sh
					$2b_1 \rightarrow 3s$	
13.7		13.8		12.70	$3a_1 \rightarrow 3p$	13.2
14.7		14.5	14.5	14.20		14.7
16.7		16.4		15.60	$2a_1 \rightarrow 3s$	15.6(c)
		18.9	19.0sh			16.5

Tabelle 2

Molecule		Single Crystal (d, f)							
vapour (a)	Solution in (c) n-heptane	$\underline{E} \parallel \underline{b}$ (001)		$\underline{E} \parallel \underline{L}$ (010)		$\underline{E} \perp \underline{L}$ (010)		$\underline{E} \parallel \underline{M}$ (010)	
		absorption R (d)		ϵ_2	R	ϵ_2	R	ϵ_2	R
${}^1B_{1u}$ 3.45±0.1 (b)	3.27 1L_a	3.14 ± 0.03	(e)	-	3.13sh			3.15±0.03	3.13
		3.32		3.31	3.30	not		3.27	3.29
		3.51		3.52	3.50	measured		3.48	3.45
		ϵ_2 (d)							
${}^1B_{2u}$ 5.24	4.84 1B_b	4.58±0.03	4.55	4.56±0.03	4.70	4.85sh	4.7	4.93±0.03	4.75
5.28 0.16		4.71	4.70		4.80				
5.40 0.16			4.90		4.95				
5.56									
${}^1B_{1u}$ ~5.8	5.62 1C_b	5.48±0.05	5.48			5.55±0.05	5.5	5.56±0.05	5.55
5.94		~6.0	5.90sh						
${}^1B_{1u}$ ~6.9	6.66 1B_a	6.33±0.1	6.40			6.30±0.1	6.33	6.30±0.1	6.33
${}^1B_{3u}$						7.05±0.1	7.1	~7.0	7.05sh
${}^1B_{1u}$ ~8.1		7.6±0.1	7.74		7.80	7.6±0.1	7.65	7.5±0.1	7.63
			9.25		~9.6				9.70
			10.4						10.65

Table 3

Oscillator strength of the ${}^1B_{2u}$ long axis polarized transition in anthracene at 4 to 5.5 eV

Vapour	Solution	Solid
$f = 0.93$ (a)	$f = 2.28$ (e)	$f_L \approx 5/3$ (i)
$f = 1.66$ (b)	$f = 1.60$ (f)	
$f = 1.6$ (c)	$f = 1.2-1.4$ (g)	
$f = 1.4$ (d)	$f = 1.5-1.6$ (h)	

Table 4


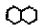
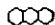

Compound	vapour		solution	solid	
	energy loss	optical		optical	energy loss
benzene 	6.2 ${}^1B_{1u}$ (a) 6.92 ${}^1E_{1u}$	6.07 ${}^1B_{1u}$ (b,c) +vibr. 6.94 ${}^1E_{1u}$ +vibr.	5.87 pure liquid (d) 6.5	polycrystalline films 5.77 (f) 6.26 (g)	polycrystalline films 6.33 (m)
naphthalene 	4.8 sh ${}^1B_{1u}$ 6.09 ${}^1B_{2u}$	4.45 ${}^1B_{1u}$ (b,c) 5.89 ${}^1B_{2u}$ +vibr.	4.45 1L_a (e) 5.70 1B_b		
anthracene 	3.45 B_{1u} 5.24 B_{2u}	3.433 ${}^1B_{1u}$ (n) +vibr. 5.24 ${}^1B_{2u}$ (b,c) +vibr. 5.8 ${}^1B_{1u}$ 6.9 ${}^1B_{1u}$ 8.1 B_{1u}	in n-heptane 3.27 1L_a (e) 4.84 1B_b 5.62 1C_b 6.66 1B_u	3.13 b (001) (h) 4.56 b (010) 5.56 M (010) 6.30 M (010) 7.5 M (010)	ϵ_{xx} ϵ_{yy} ϵ_{zz} (g) 3.3 3.3 4.65 5.7 6.6 6.6 8.2 7.9 10.2 10.8 15.3 15.3 15.0
tetracene 	2.7 ${}^1B_{1u}$ 4.65 ${}^1B_{2u}$ 6.07		2.6 (e) 4.7 5.9	2.46 a, 2.39 b (i) 4.6 b 5.71 a, 5.64 b	

Table 4 continued

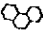
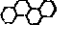

phenanthrene 	5.20 6.6 sh		4.88 B _b (e) 6.62 B _a		5.0 4.7 5.1 (k) 7.1 7.0
chrysene 	4.80 ¹ B _u 6.9		4.61 B _b (e) 6.73 C _a	4.56 a, b (001) (i)	4.6 4.6 4.6 (k) 6.8 6.5
pyrene 	4.04 5.28 6.59		3.7-3.8 ¹ L _a (e) 4.6 ¹ B _a 5.2 ¹ B _b 6.3	3.67 b (i) 4.60 a, 4.54 b 5.2 a	3.7 4.5 4.6 (1) 5.2 6.5 6.55

Figure Captions

- Fig. 1 Sketch of the monochromator with absorption cell cut perpendicular to the synchrotron plane (Ref. 17)
(TMP turbo molecular pump, DP diffusion pump, VP fore pump, V valve, DV needle valve, RV reduction valve, TV gate valve, SR beam pipe, SY synchrotron radiation, SB apertures, G grating, DA excentric pivot, WLT wavelength drive, Fi filter, AS exit slit, A absorption cell, S sample, M_1 , M_2 pressure gauges, LS sodium salycilat screen, F window, PM photomultiplier)
- Fig. 2 Sketch of the monochromator with reflectometer cut perpendicular to the synchrotron plane (Ref. 17)
- Fig. 3 Sketch of the electron energy loss spectrometer
(K cathode, HV high voltage power supply, AN anode, AP aperture, FL focusing lens, OS target solid samples, OV target gaseous samples, ESA electrostatic deflection field, A Möllenstedt type analyzer, S slit, M magnetic deflection field, PM photomultiplier, W window, SBD surface barrier detector, DCR DC-recording, R recorder, MCA Multi channel analyzer)
- Fig. 4 Comparison of the energy loss spectrum of 30 keV electrons (solid line and dashed line³⁶) and the optical absorption spectrum⁸⁶ of gaseous benzene for excitation energies 4 to 30 eV.
- Fig. 5 Comparison of the optical absorption spectrum (solid line⁸⁴) and the energy loss spectrum of 100 eV electrons (dashed line⁸⁰) of gaseous benzene for photon energies 7.5 to 14.5 eV.

- Fig. 6 Qualitative description of directional dispersion of a single exciton, as probed by electron spectroscopy and normal incidence reflection spectroscopy. The shaded area corresponds to the reflection bands (see text).
- Fig. 7 Absorption spectra of methane, ethane, propane and butane for the range of excitations from the σ -valence shell electrons (solid line²⁶). Results from Ref. 50 for methane, ethane, and butane are given too (dashed line).
- Fig. 8 Absolute absorption cross sections for methane and ethane (solid line) and reflectance for solid films of methane and ethane²⁶.
Dots: Ref. 71
- Fig. 9 Absorption spectrum of benzene vapour from 5 to 35 eV (Ref. 85)
- Fig. 10 Absorption spectrum of benzene vapour in the spectral range 9 to 14 eV (Ref. 85)
- Fig. 11 Absorption spectrum of benzene and perdeuterobenzene in the spectral range 14 to 18 eV (Ref. 85)
- Fig. 12 Reflectance from polycrystalline films of benzene (solid line, Ref. 17). results from Ref. 00 and the vapour spectrum are shown by dashed lines.
- Fig. 13 Densitometer trace of the naphthalene absorption spectrum in the 7.5 eV range. Position of absorption bands are given in eV. The incoming intensity is constant over this range. Arrows indicate structures assigned to antiresonances in Ref. 109.

- Fig. 14 Densitometer trace of the absorption spectrum of anthracene vapour from 5 to 8.5 eV. The incoming intensity is nearly constant over this range. Indicated Rydberg series have been calculated with the given quantum defects, values for the ionization potentials are taken from Ref. 116.
- Fig. 15 Electron energy loss spectrum of 30 keV electrons in anthracene vapour (dashed line). The solid line gives the normalized spectrum.
- Fig. 16 Projection of the anthracene unit cell onto the ac- and ab-plane and the projections of the normalized transition moments for long (L_1, L_2) and short (M_1, M_2) axes polarized transitions lying in the molecular plane and for the normal axes (N_1, N_2) together with the projections of the sum and differences of these.
- Fig. 17 Reflectance of anthracene single crystals for s-polarized light at near normal incidence (7.5°) from the (001)-plane for $\underline{E} \parallel \underline{b}$ and for the (010)-plane for $\underline{E} \parallel \underline{L}$ and $\underline{E} \perp \underline{L}$ and dielectric functions deduced from it.⁶⁰
- Fig. 18 Spectra for n_{eff} of anthracene single crystals for three polarization directions, as obtained from a Kramers-Kronig analysis of reflectance data.
- Fig. 19 Normal incidence reflectance spectra ($\theta = 0^\circ$) of anthracene single crystals for various artificially prepared planes with $\underline{E} \perp \underline{b}$ according to Hymowitz and Clark¹²² (solid line) compared to calculated reflectance using ϵ -values derived from (010) reflectance data (broken line). The orientations of the reflecting planes are given as inserts.⁶⁰

- Fig. 20 Comparison of the energy loss function $|\text{Im } \epsilon^{-1}|$ as obtained from the optical data (solid line) and from energy loss experiments by Venghaus¹³¹ (dashed line).
- Fig. 21 Several electron energy loss spectra in the lower energy range for different \underline{k} directions in the \underline{ac} -plane (Ref. 39)
- Fig. 22 Experimental dependence of the loss energy ΔE on the \underline{k} direction in the \underline{ac} -plane. For the direction of axis, see Fig. 16. Full circles, full squares, circles and rectangles show qualitatively the variation of the loss intensity, going from pronounced peaks over weaker peaks to shoulders and weak shoulders, respectively. Values $\Delta E(\underline{k})$ belonging to the same peak have been connected for a better general view, error limits are indicated in the left side of the figure (Ref. 39).
- Fig. 23 Experimental (a: Ref. 36) and calculated (b: Ref. 132, c: Ref. 133 d: Ref. 134) values for the $\pi-\pi^*$ excitation energies for the ${}^1B_{1u}$ short axis and ${}^1B_{2u}$ -long axis polarized transition in polyacenes. Ionization potentials (e: Ref. 116) as determined by photoelectron spectroscopy are shown too.
- Fig. 24 Energy loss spectrum of 30 keV electrons in vapour of ferrocene (dashed line). The solid line is the normalized spectrum³⁷. The black area shows the main structure of the optical absorption in solution¹⁴³.

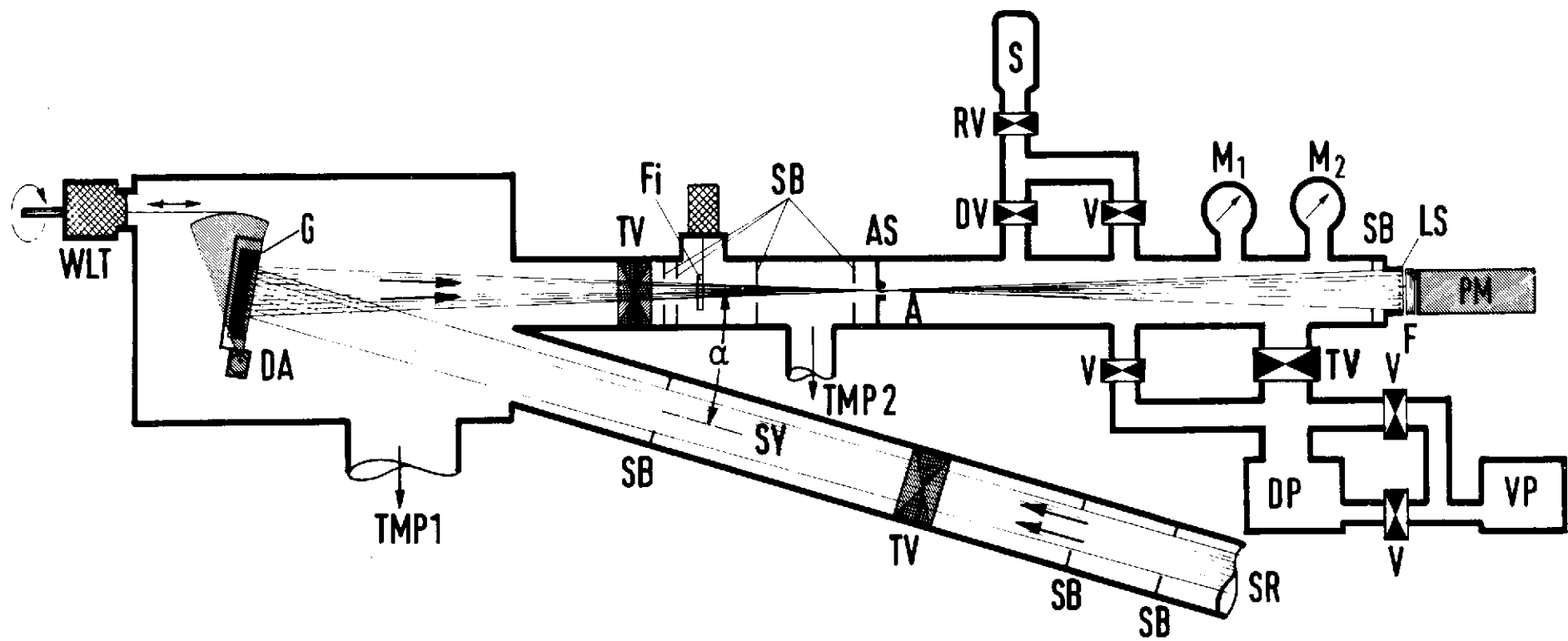


Fig. 1

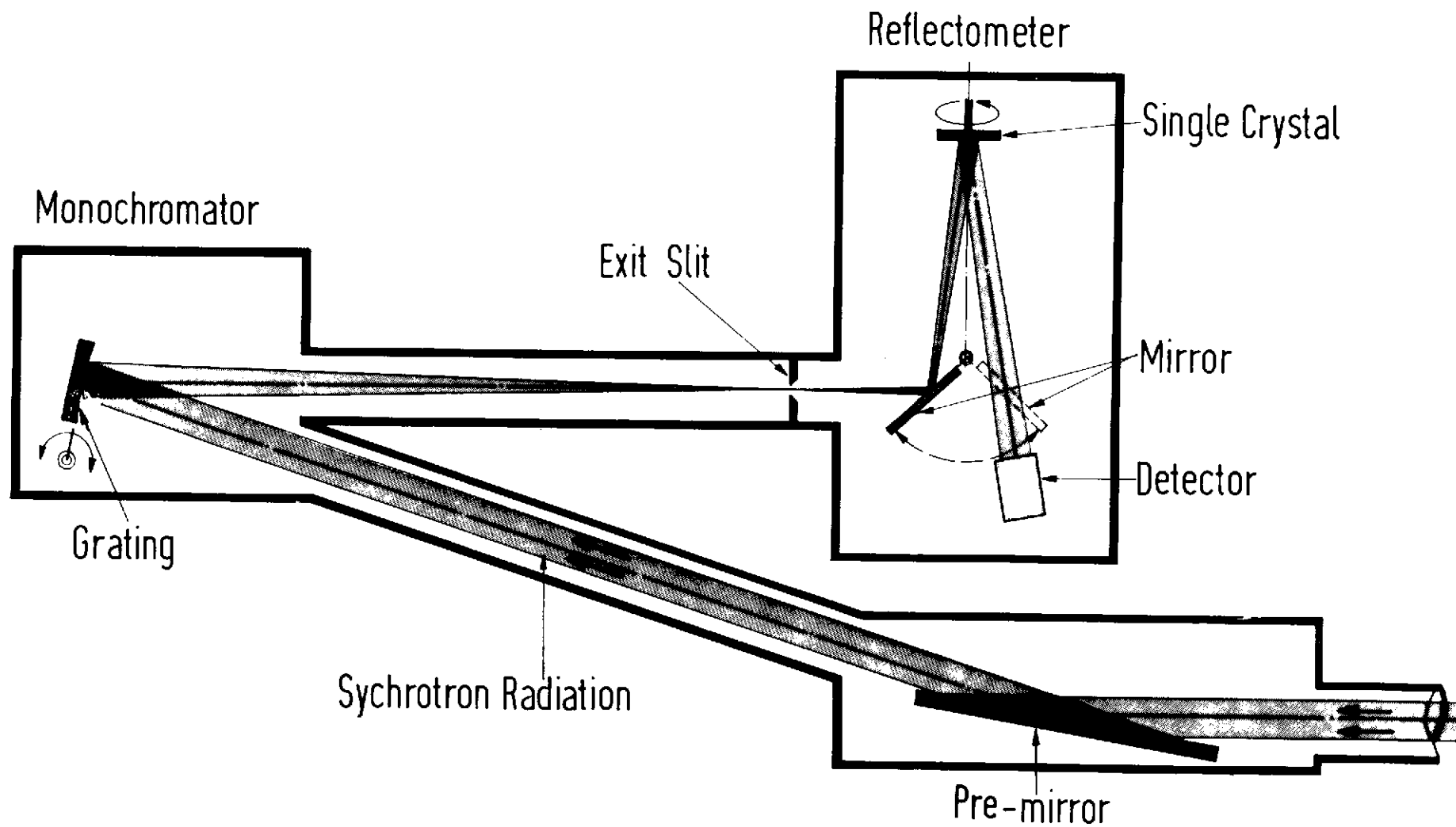


Fig. 2

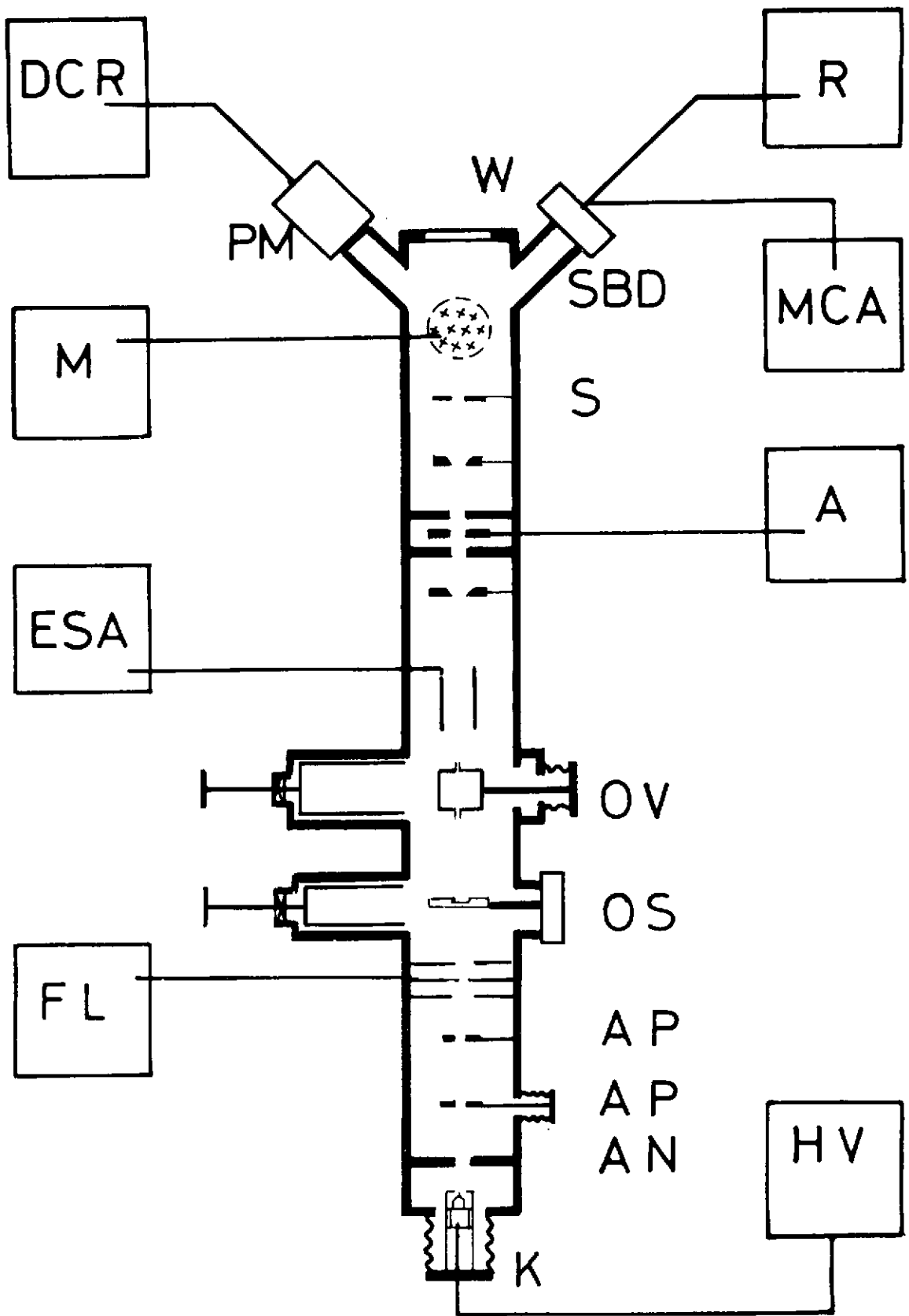


Fig.3

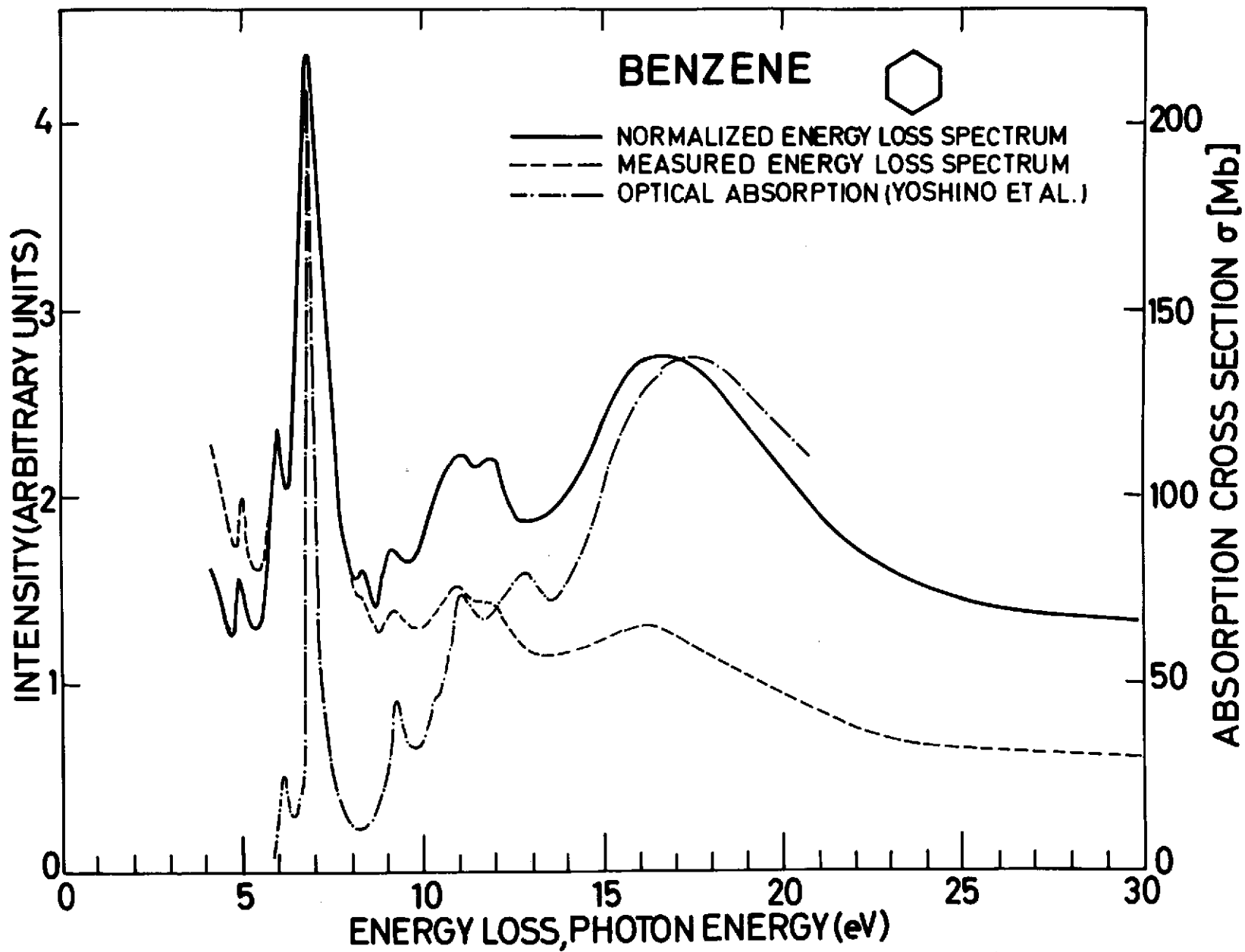


Fig. 4

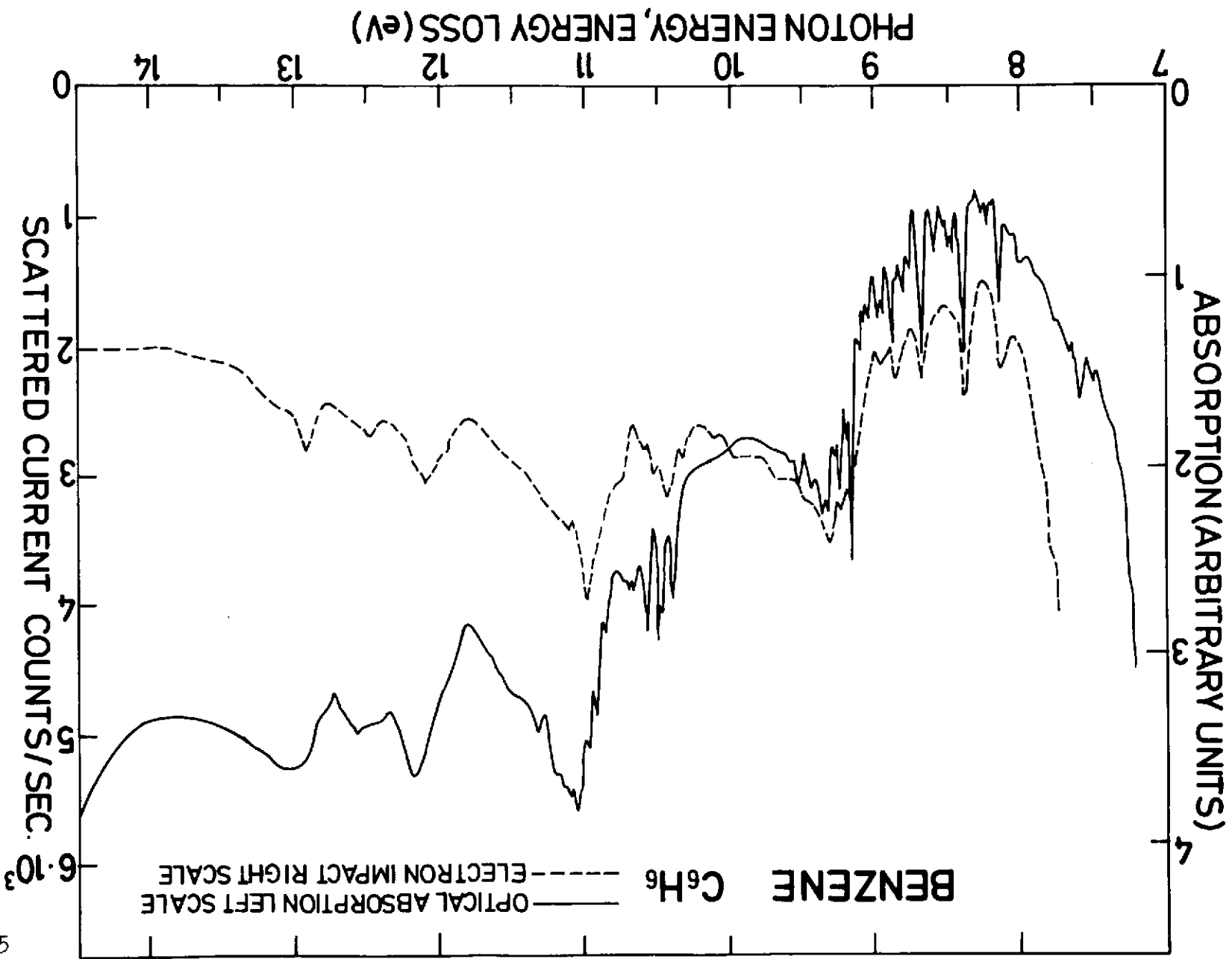


Fig. 5

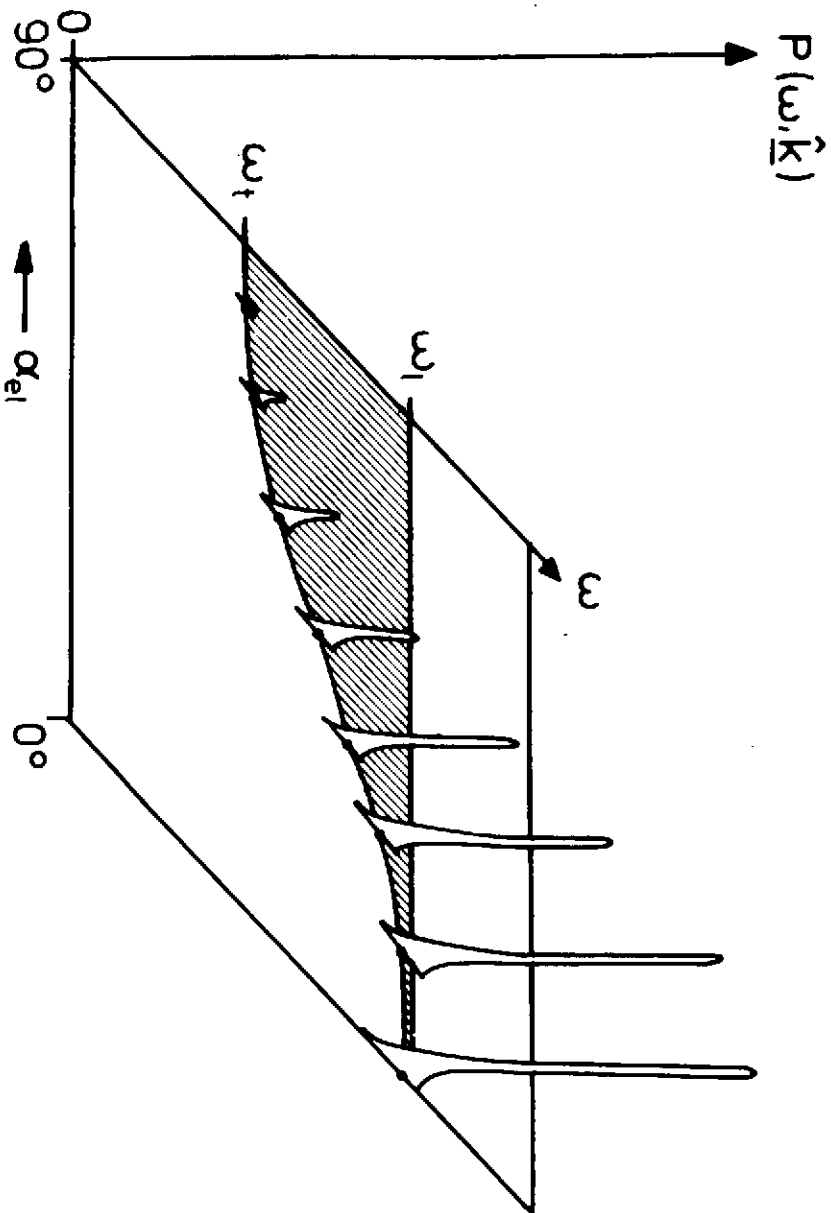
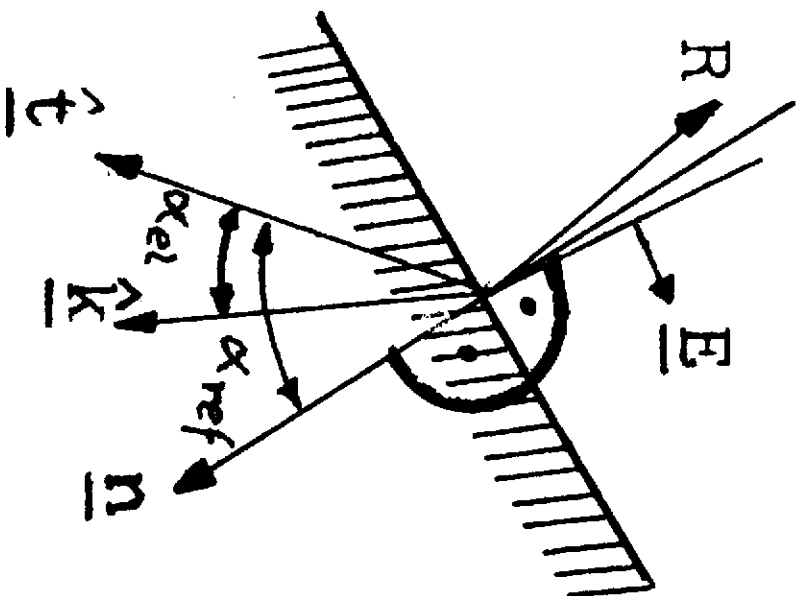


FIG. 6

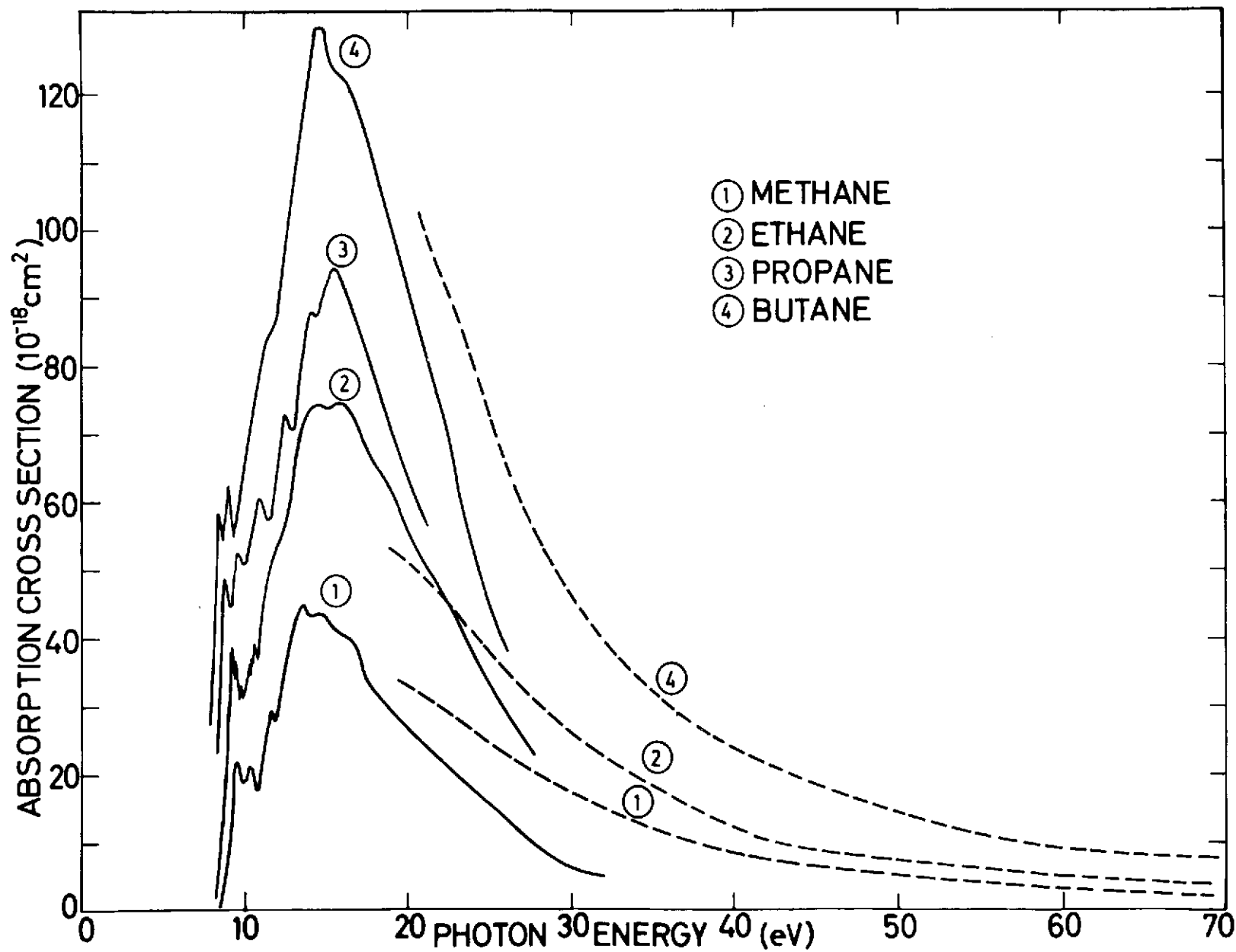


Fig.7

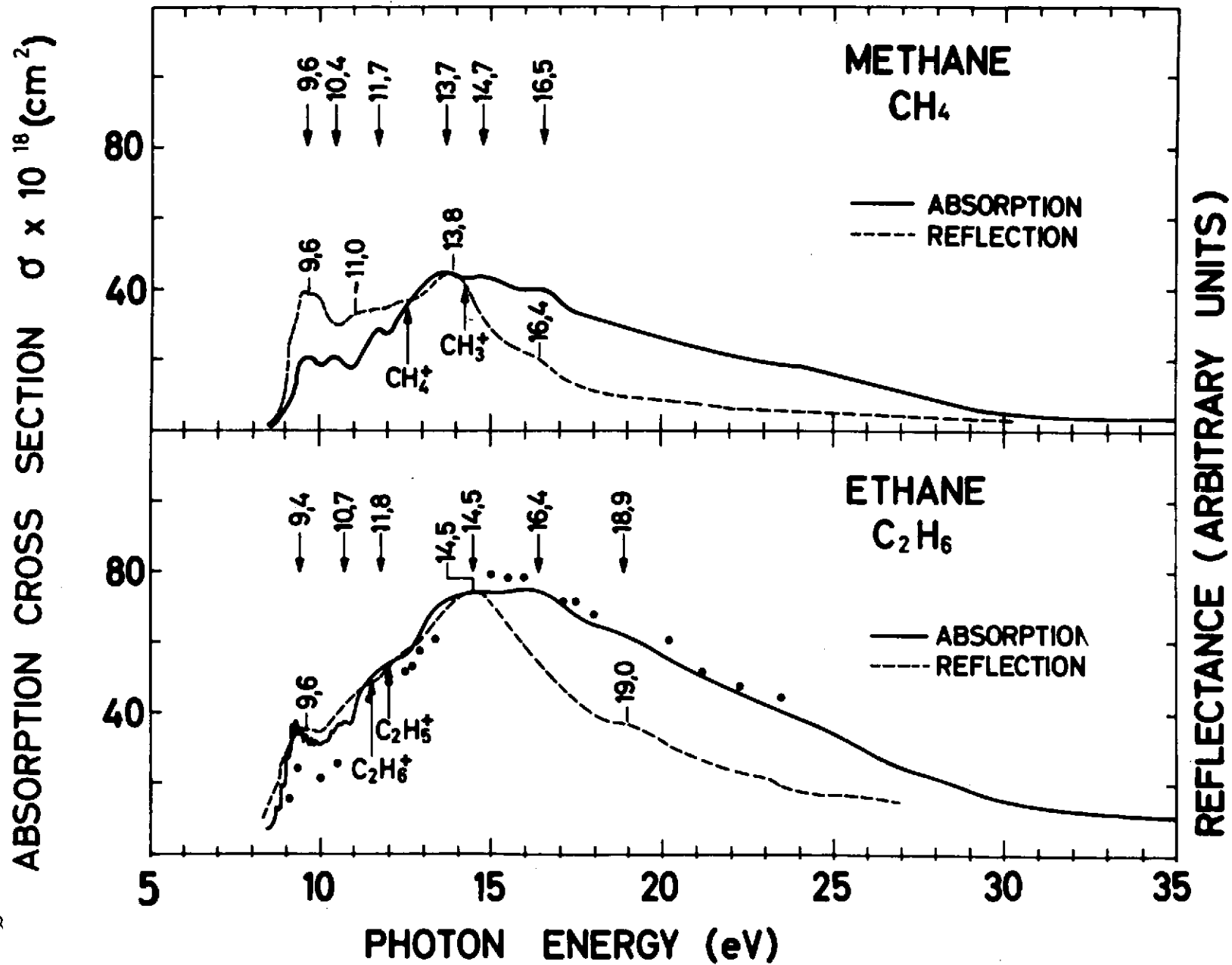


Fig.8

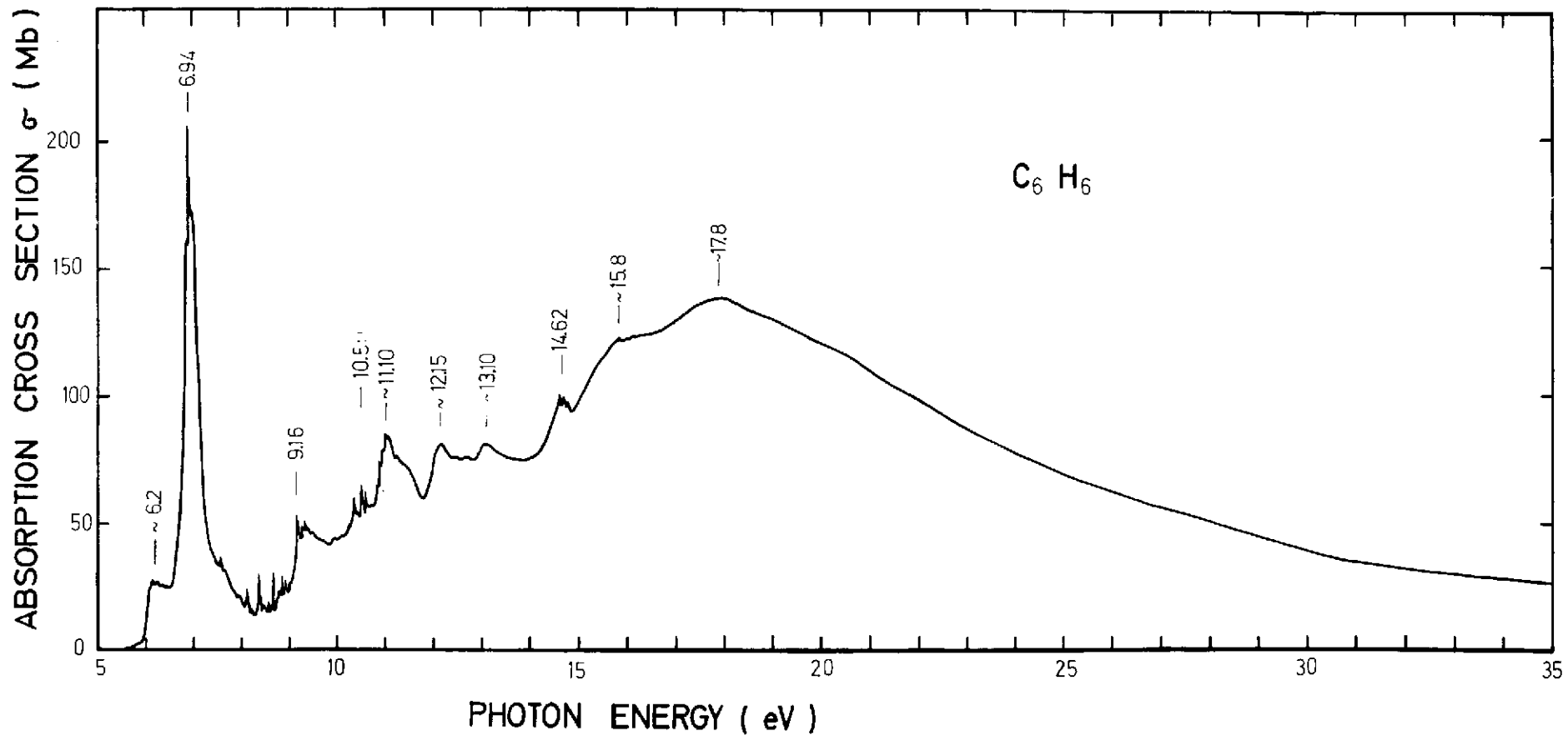


Fig. 9

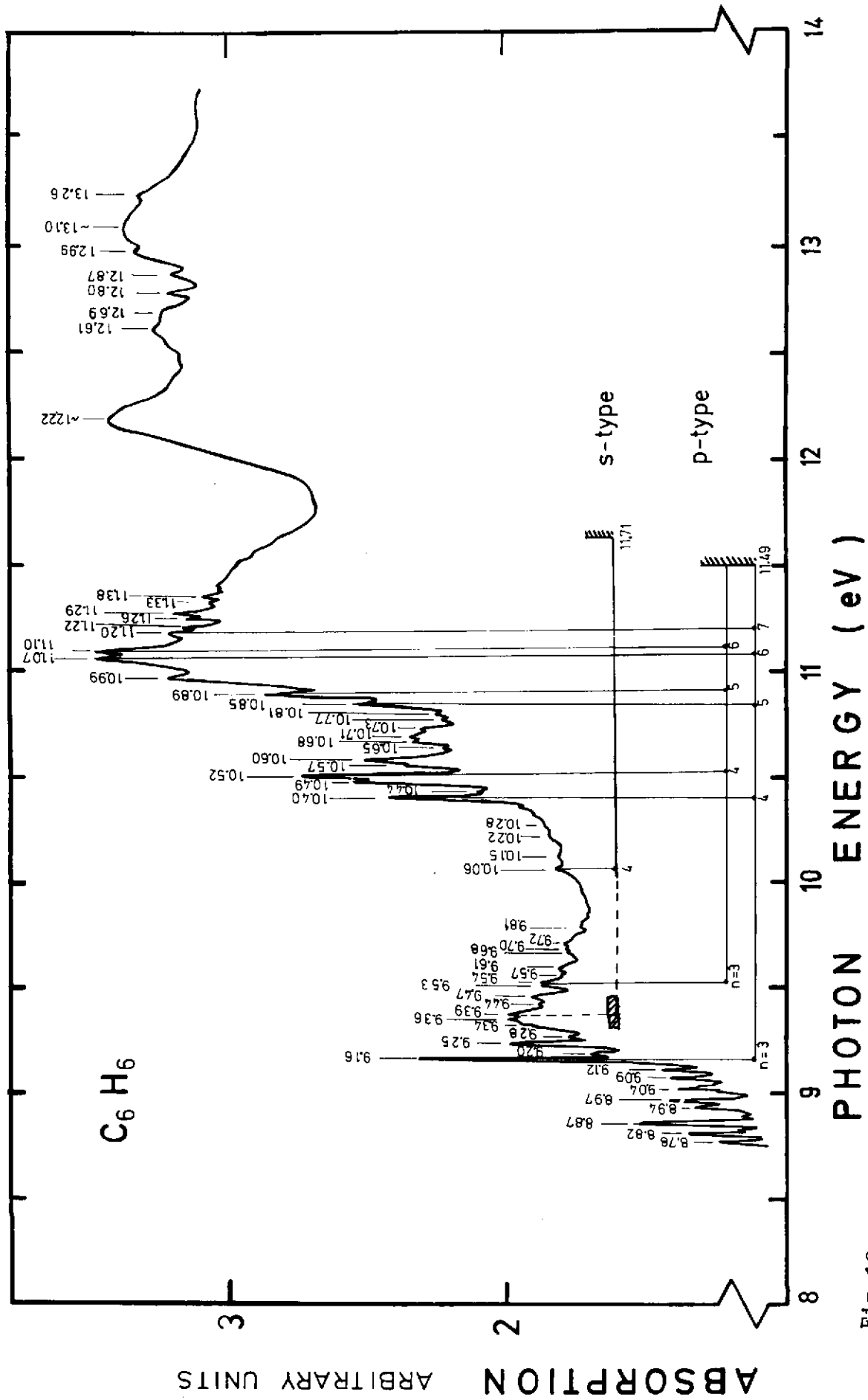


Fig. 10

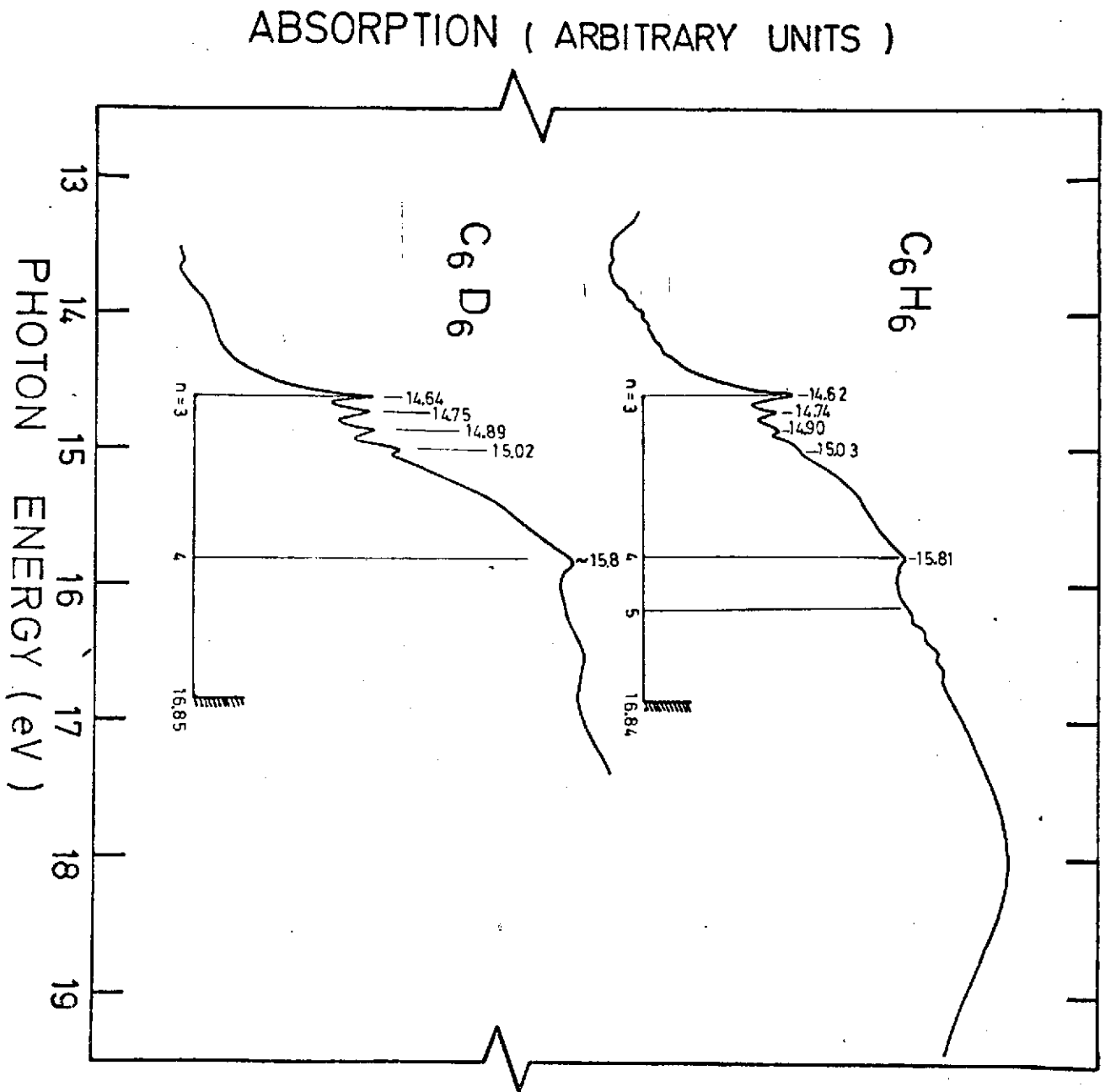


FIG. 11

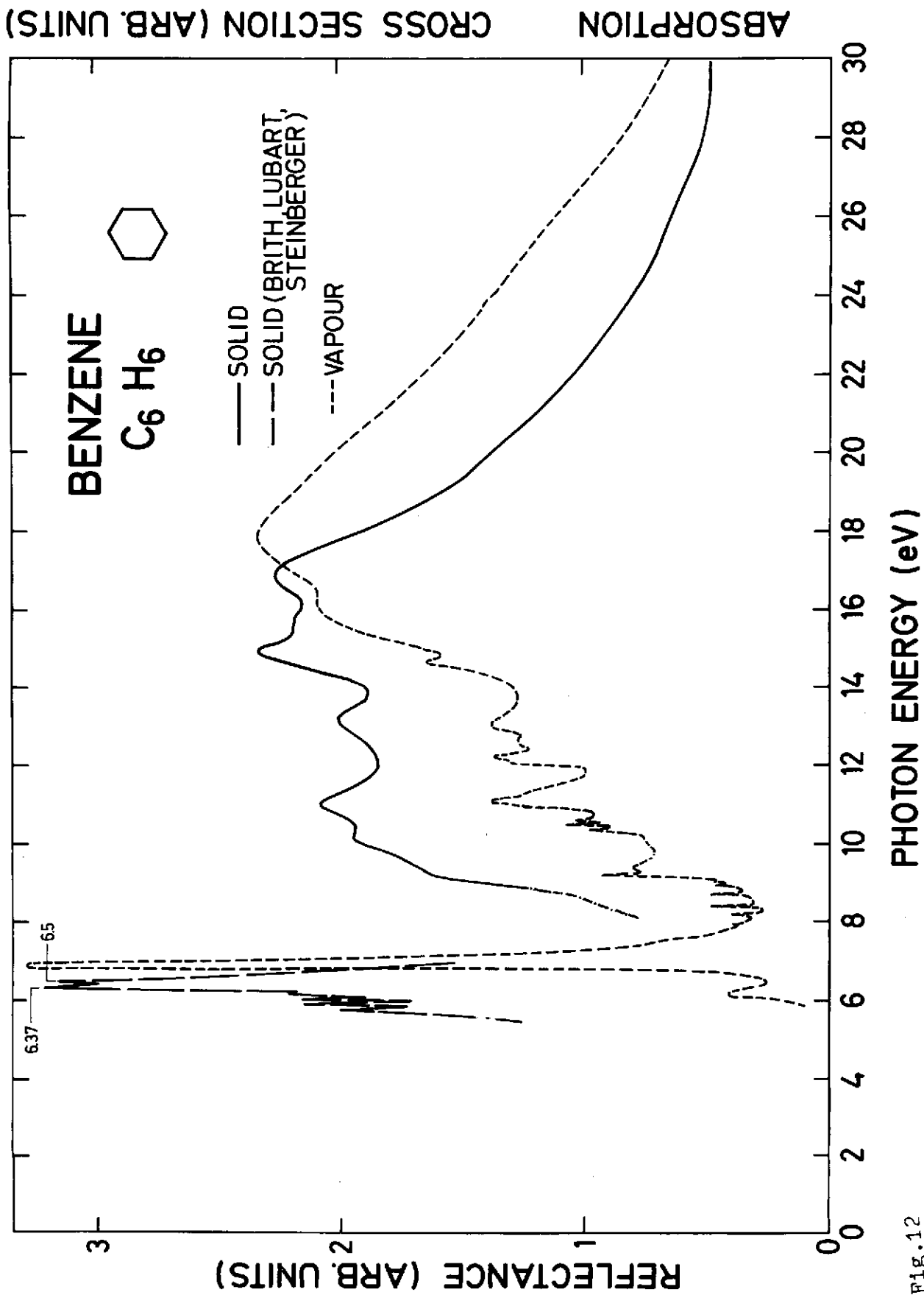


FIG. 12

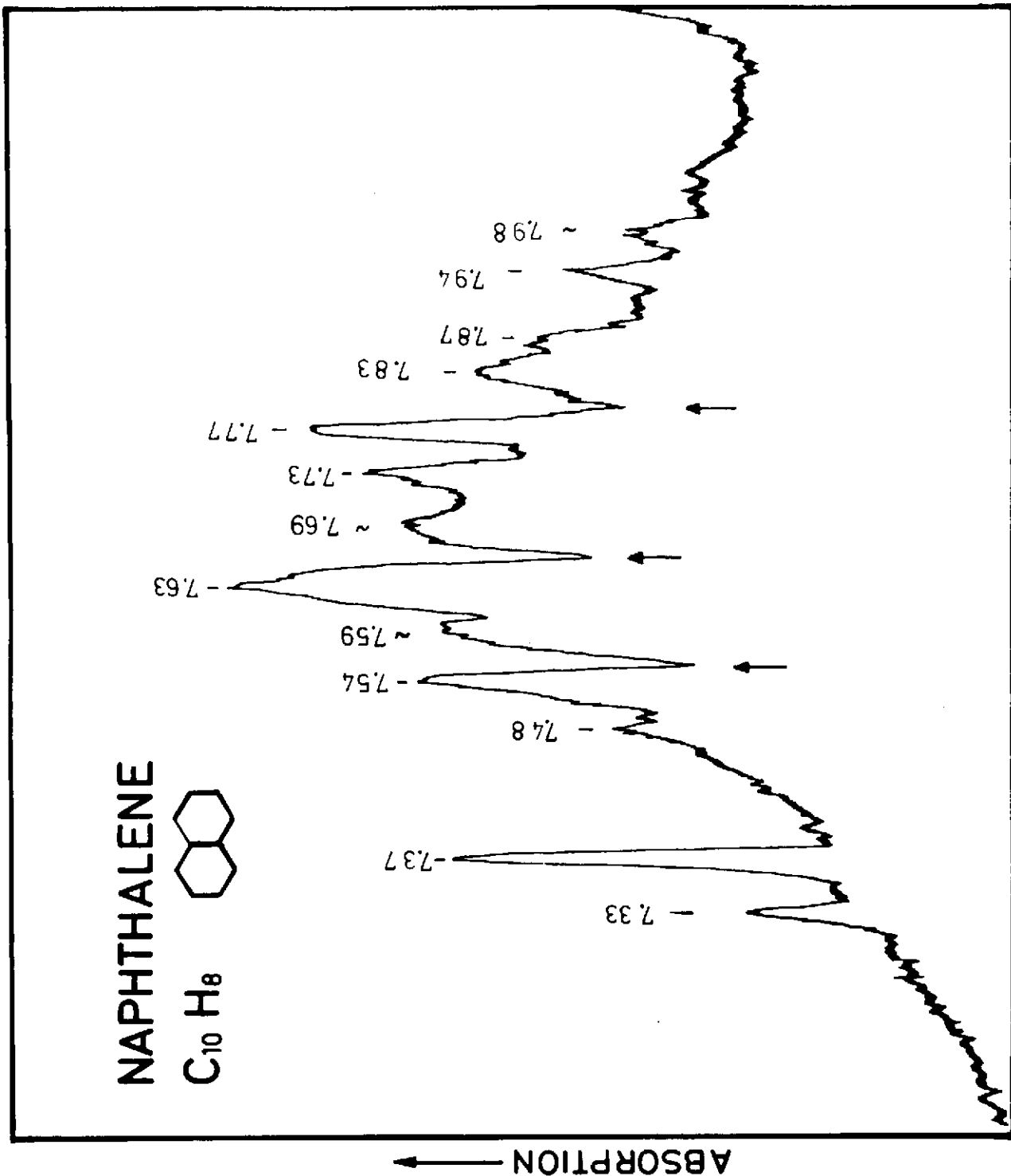
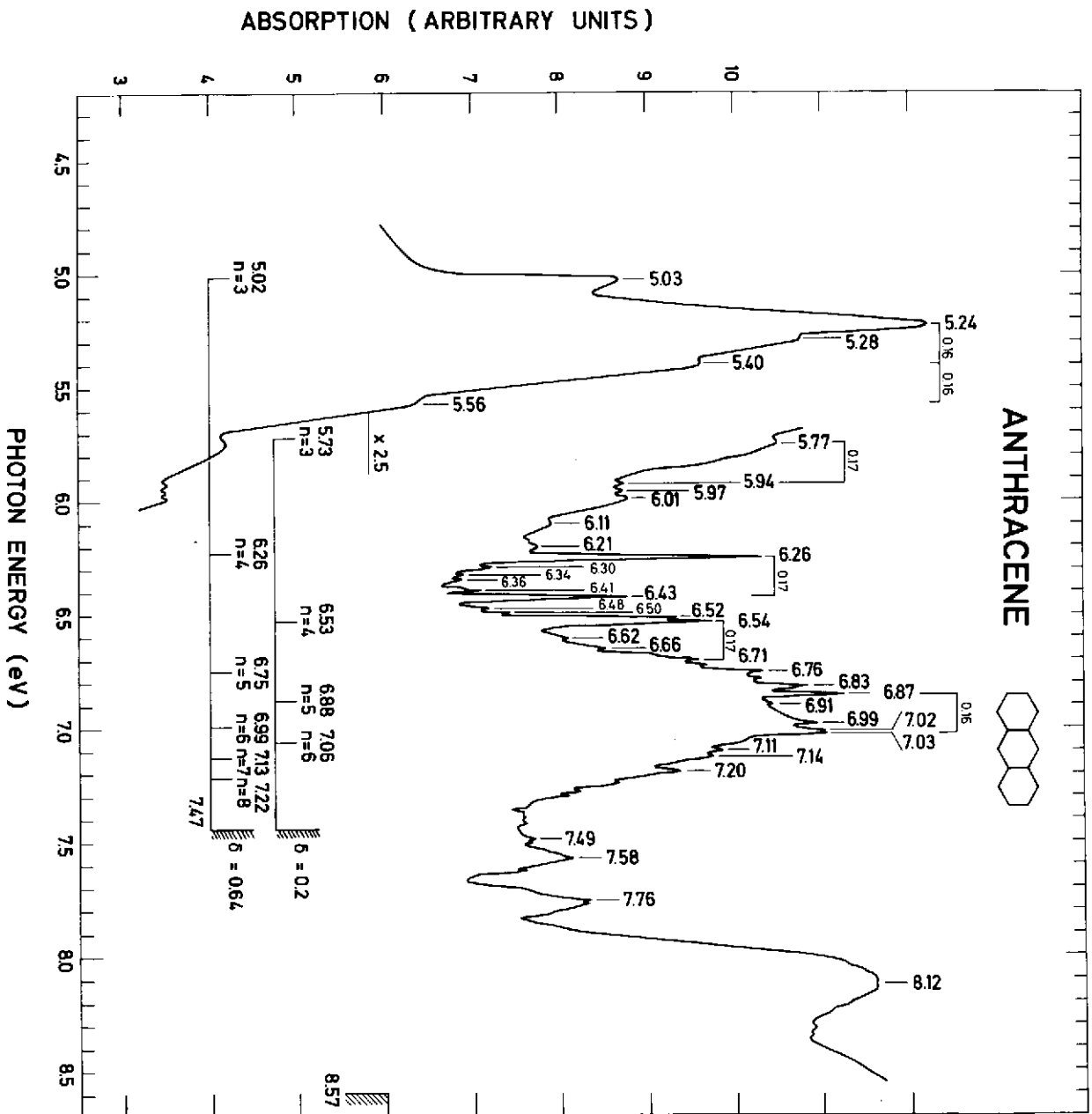


FIG. 13



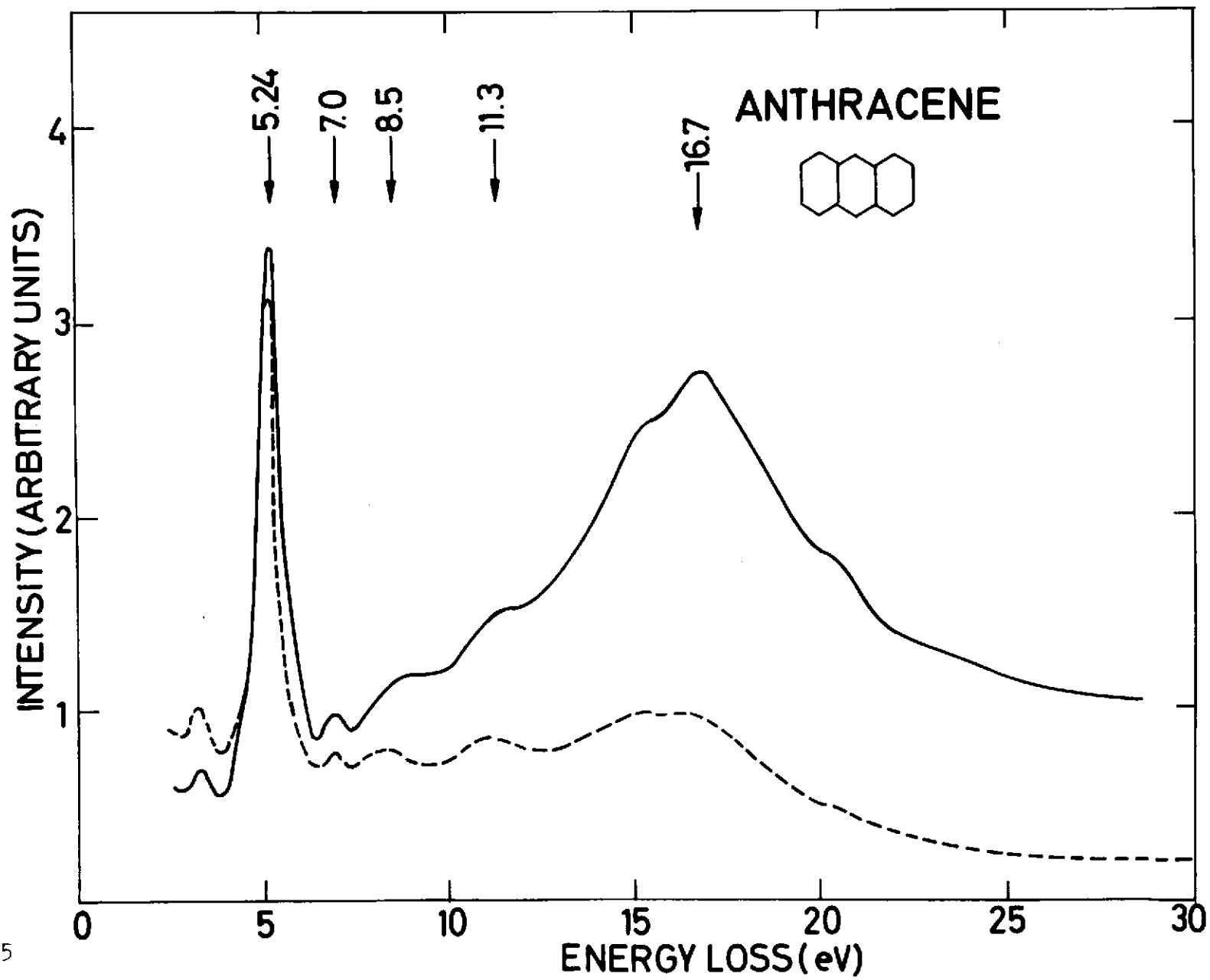


Fig.15

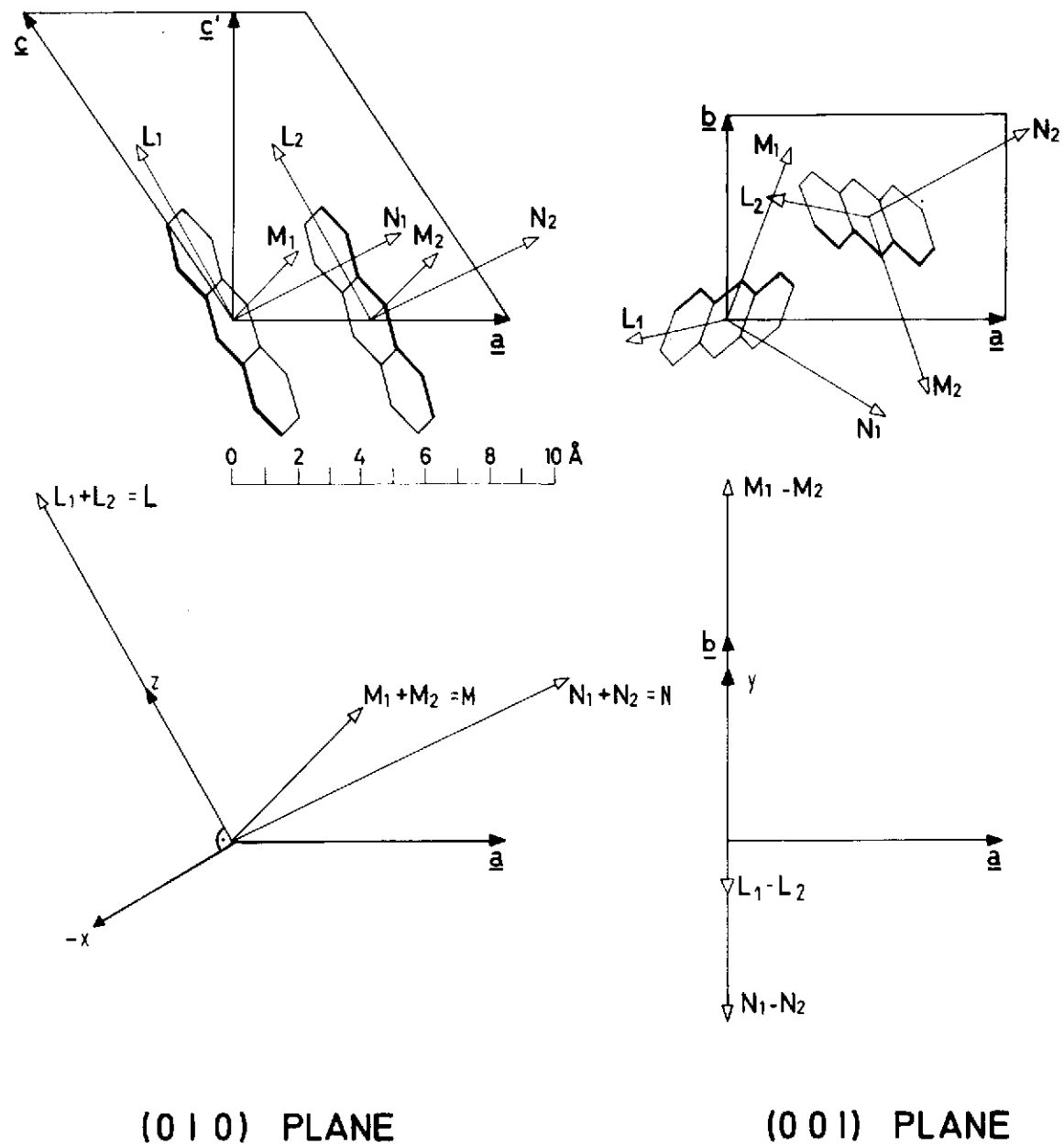


Fig.16

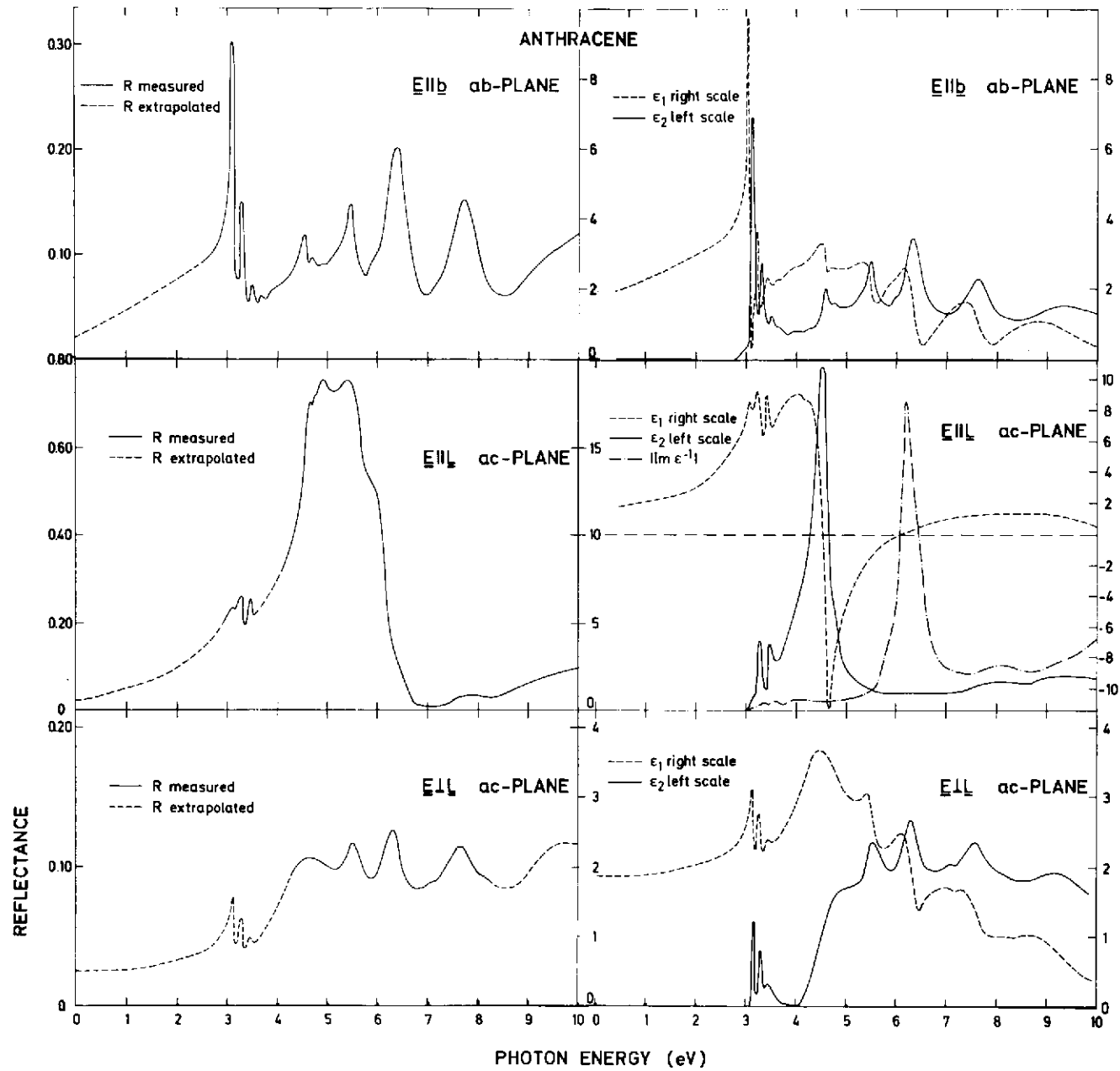


Fig.17

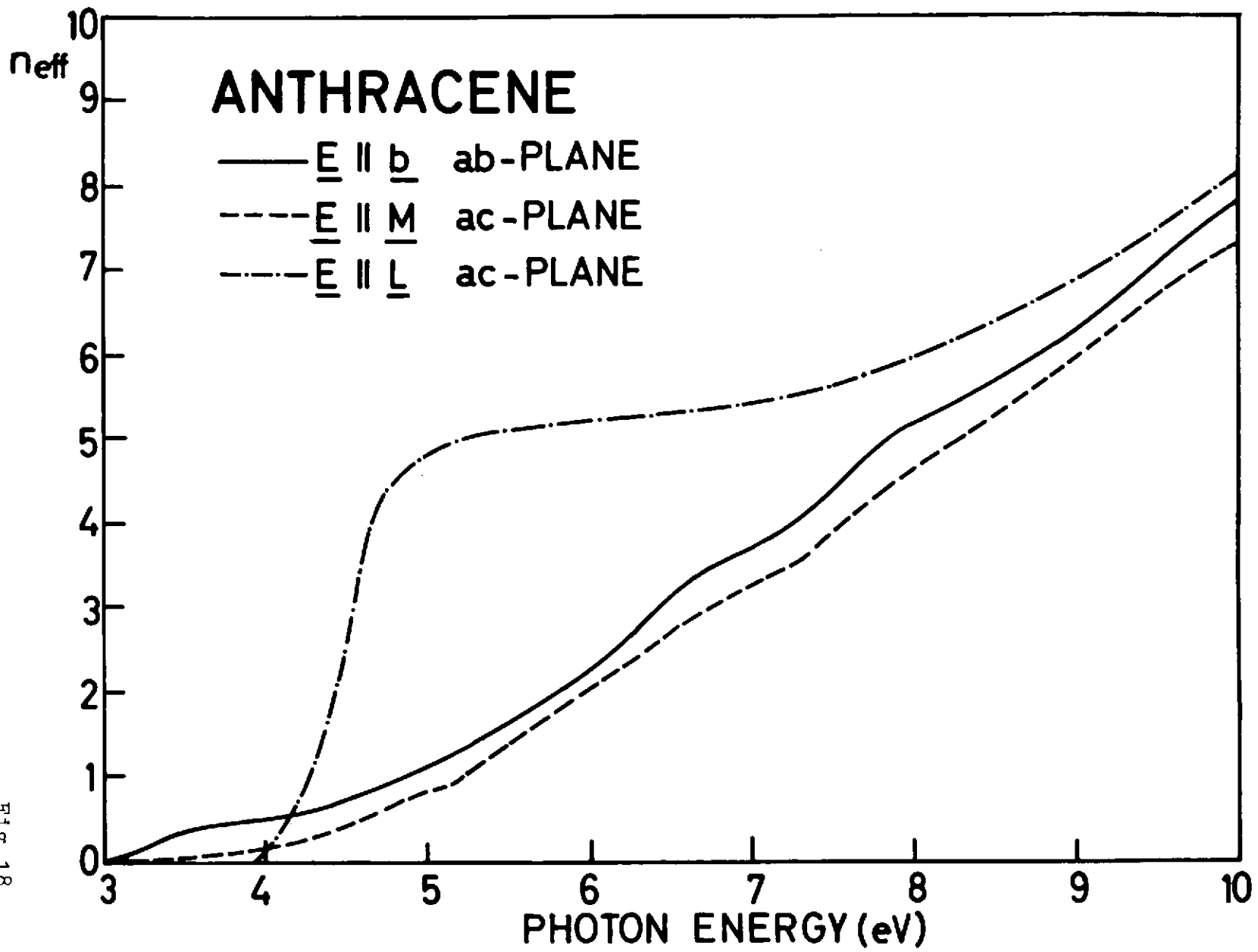


FIG. 18

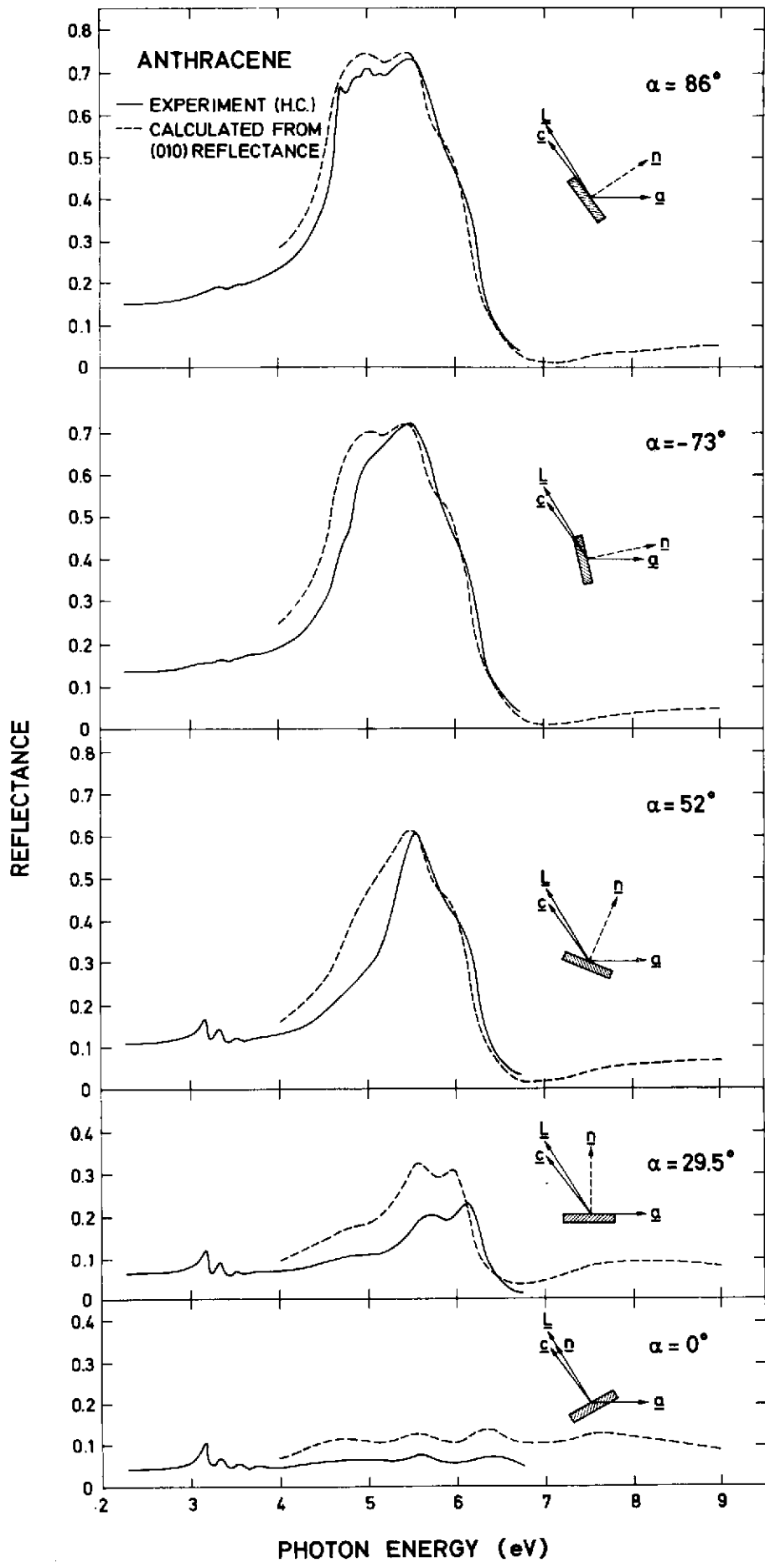


FIG. 19

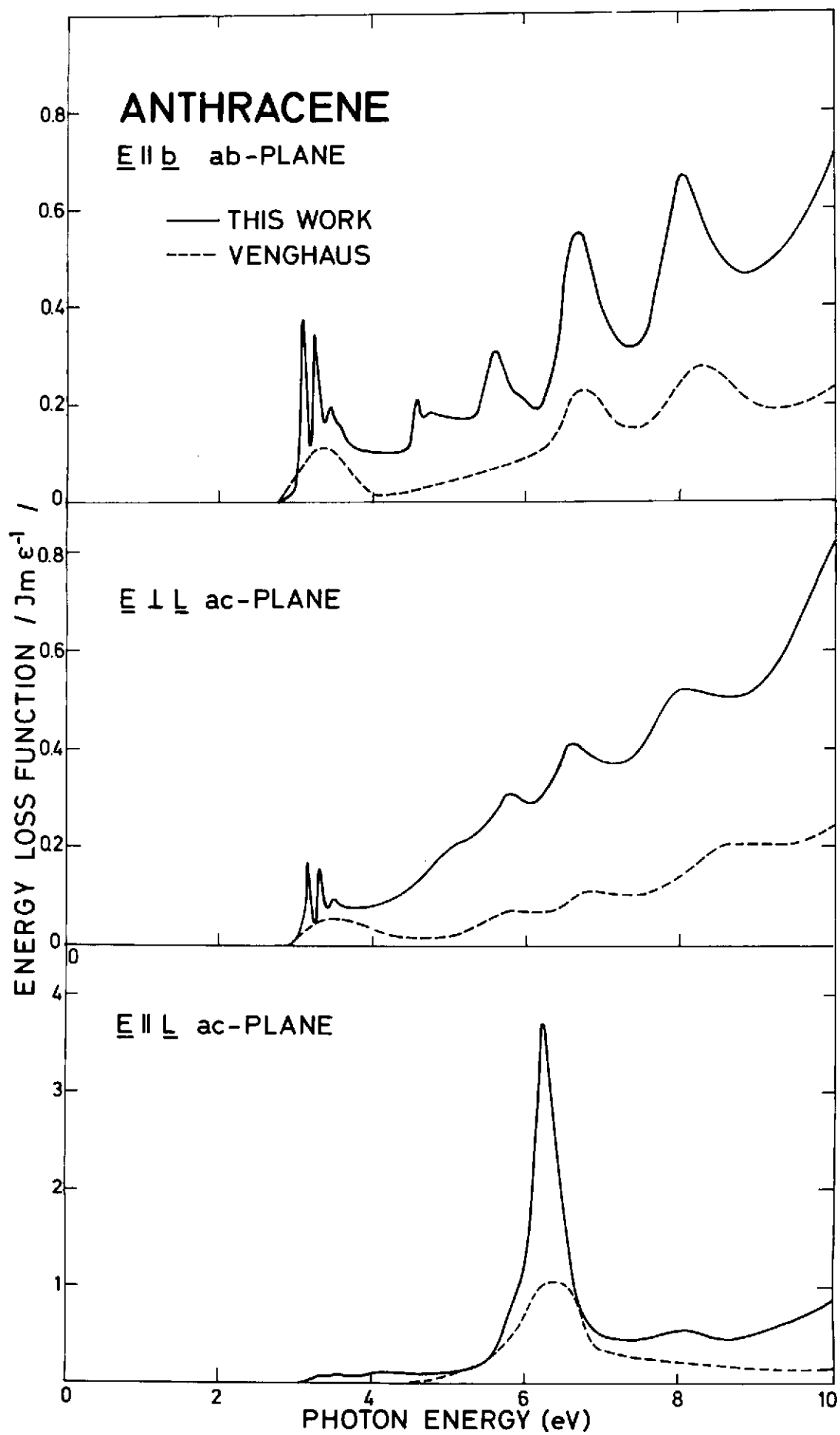


Fig. 20

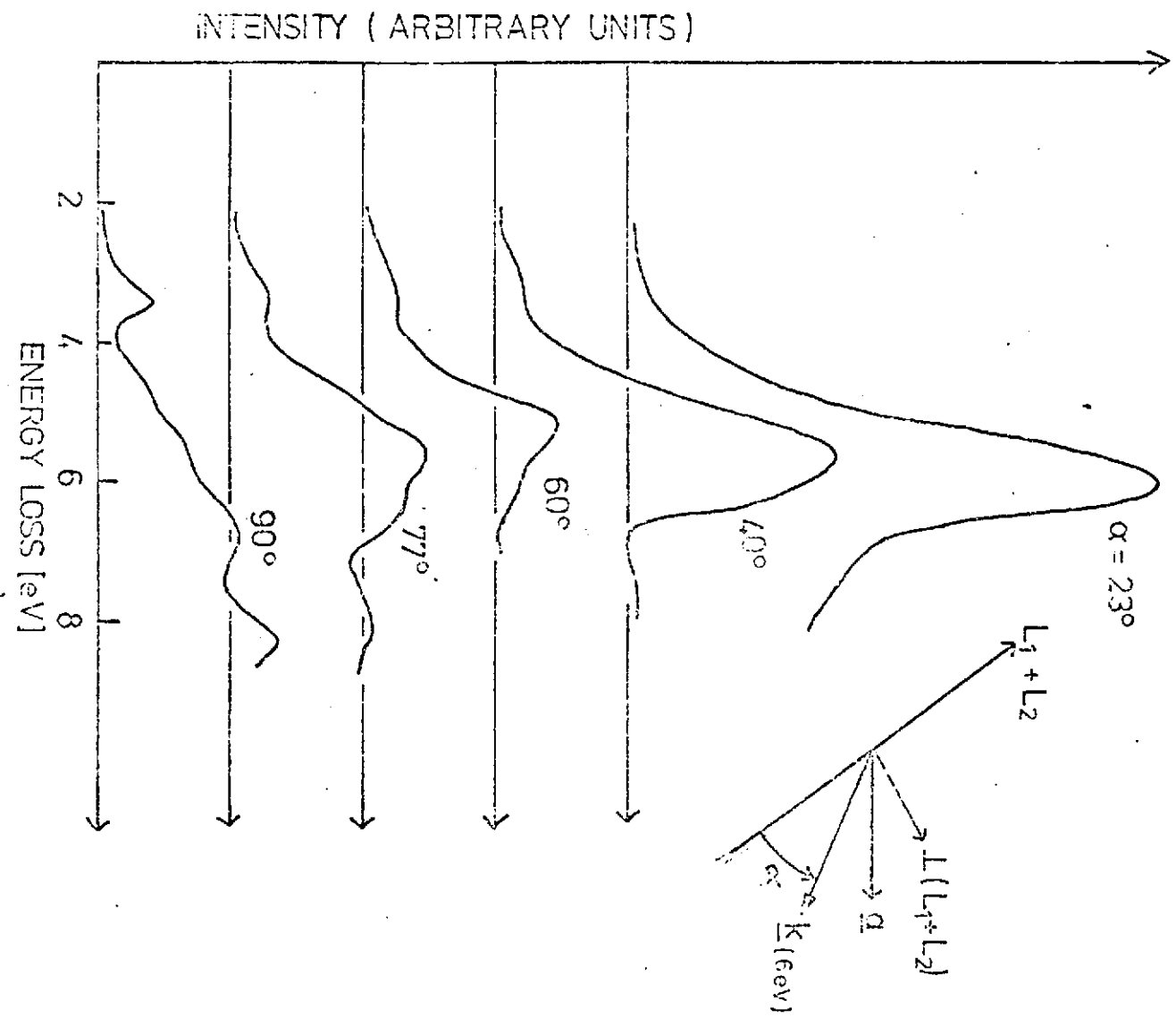


FIG. 21

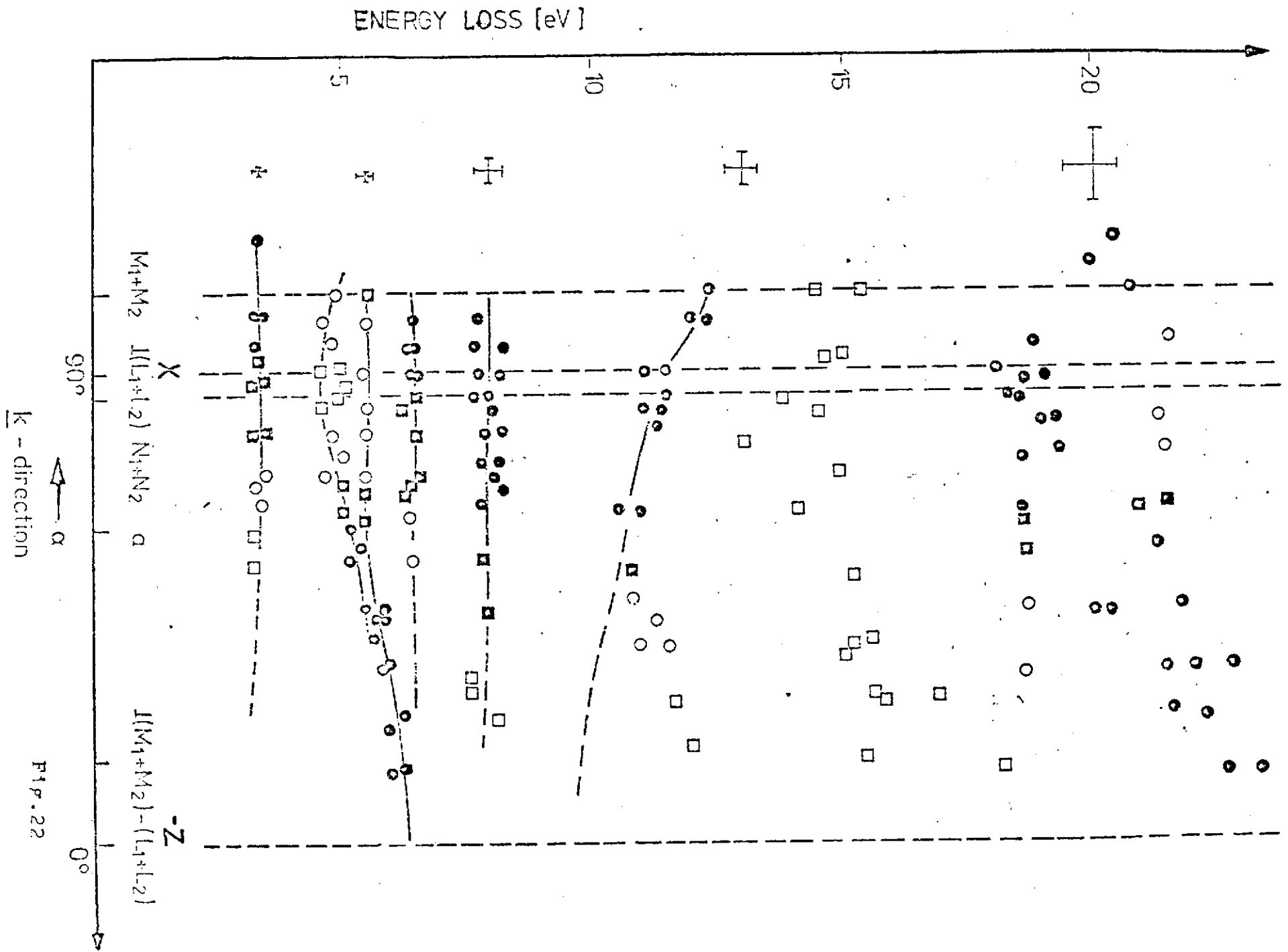


Fig. 22

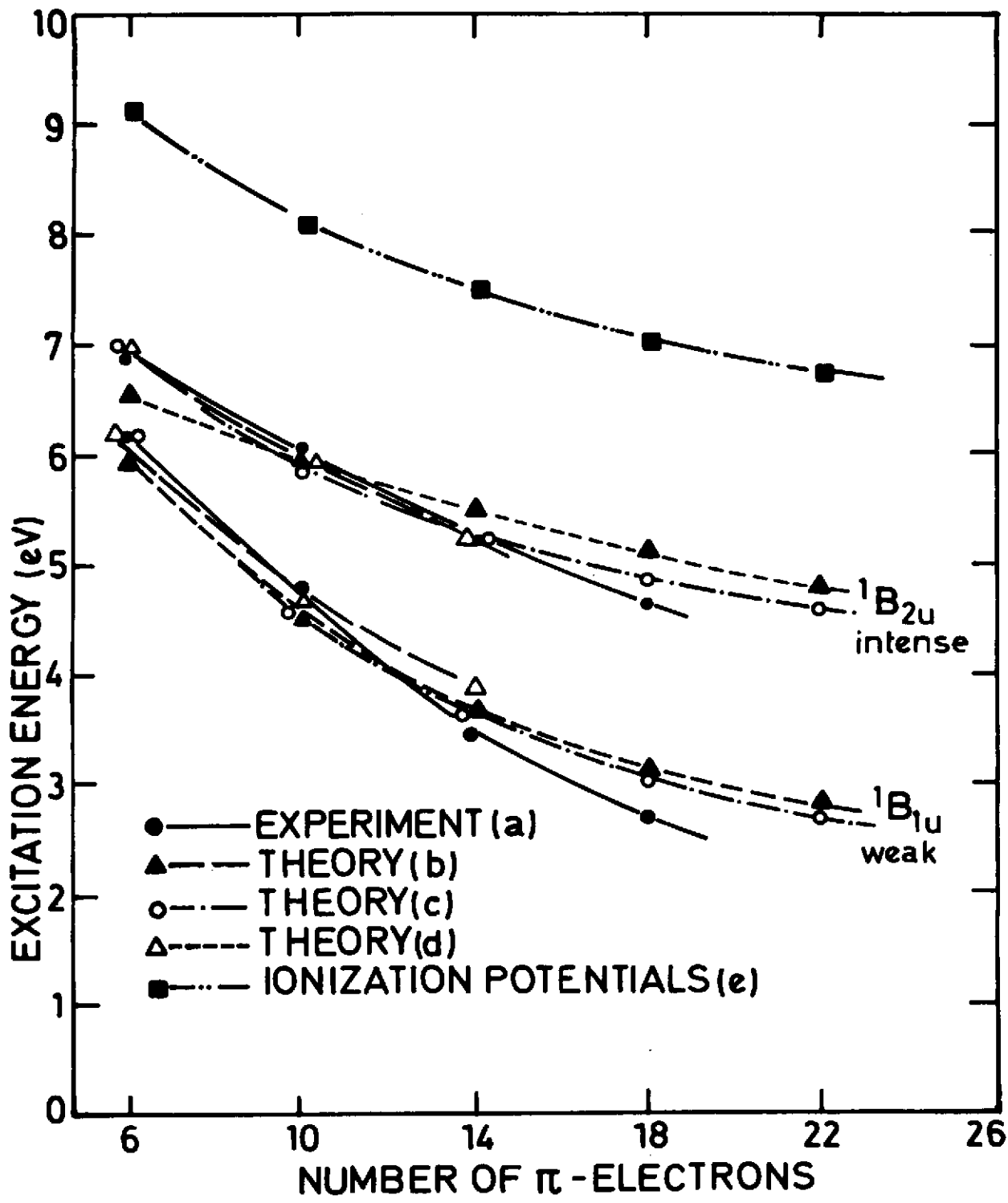


Fig.23

